

AN INVESTIGATION OF THE FEASIBILITY
OF APPLYING FREQUENCY RESPONSE ANALYSIS
TO STUDY FLUID FLOW REACTORS

By

HAROLD S. HORNECK, B.A.Sc.

A Thesis

Submitted to the Faculty of Graduate Studies
in Partial Fulfilment of the Requirements

for the Degree

Master of Engineering

McMaster University

September 1970

MASTER OF ENGINEERING (1970)
(Chemical Engineering)

McMASTER UNIVERSITY
Hamilton, Ontario

TITLE: An Investigation of the Feasibility of Applying
Frequency Response Analysis to Study Fluid
Flow Reactors

AUTHOR: Harold Stevenson Horneck, B.A.Sc. (University of Windsor)

SUPERVISOR: Dr. J. D. Norman

NUMBER OF PAGES: viii , 117

SCOPE AND CONTENTS:

A frequency response tracer technique was used to study the hydraulic properties of a laboratory flow through reactor with variations in reactor size , flow rate and applied mixing. At any one set of conditions the reactor was studied over a range of input sine wave frequencies. Theoretical models consisting of in-series networks of completely mixed segments , plug flow segments , and dead space allowances were developed to approximate the experimental findings.

ACKNOWLEDGEMENTS

I wish to thank Dr. J. D. Norman for his assistance and guidance during the course of the research work and in the preparation of this thesis.

Thanks are also due to the Ontario Water Resources Commission for the leave of absence and financial assistance provided to complete this work.

Finally , I would like to thank my wife Marion for help in typing this thesis and more especially for her patience and encouragement.

Harold Horneck

TABLE OF CONTENTS

	<u>PAGE</u>
ACKNOWLEDGEMENTS	iii
LIST OF FIGURES	vi
LIST OF TABLES	vii
CHAPTER 1 <u>INTRODUCTION</u>	1
1.1 PURPOSE AND SCOPE OF THE INVESTIGATION...	1
1.2 POSSIBLE APPLICATIONS OF THIS WORK.....	2
CHAPTER 2 <u>REVIEW OF RELATED WORK</u>	6
2.1 GENERAL STATEMENT.....	6
2.2 METHODS OF ANALYSIS.....	6
2.3 DISCUSSION.....	9
2.4 FREQUENCY RESPONSE REFERENCES.....	15
CHAPTER 3 <u>THE CONCEPT OF FREQUENCY RESPONSE</u>	19
3.1 THEORY.....	19
3.2 LINEARITY AND STABILITY.....	20
3.3 DATA ANALYSIS AND REPRESENTATION.....	22
CHAPTER 4 <u>EXPERIMENTAL METHOD</u>	30
4.1 EXPERIMENTAL EQUIPMENT.....	30
4.2 EXPERIMENTAL TECHNIQUE.....	37
CHAPTER 5 <u>DATA ANALYSIS</u>	39
5.1 AMPLITUDE RATIO.....	39
5.2 PHASE LAG.....	39
5.3 INPUT WAVEFORM.....	40
5.4 OUTPUT WAVEFORM.....	41

	<u>PAGE</u>
CHAPTER 6	<u>EXPERIMENTAL RESULTS</u> 45
6.1	GENERAL..... 45
6.2	EXPERIMENTS I AND II - NO MIXING PROVIDED..... 47
6.2.1	Models 1 and 2..... 52
6.2.2	Models 3 and 4..... 55
6.3	EXPERIMENTS I AND II - MIXING PROVIDED.. 58
6.3.1	Models 5 and 6..... 61
6.3.2	Models 7 and 8..... 61
6.4	EXPERIMENT III - NO MIXING PROVIDED..... 66
6.4.1	Model 8..... 69
6.5	DISCUSSION..... 69
6.5.1	Amplitude Ratio..... 69
6.5.2	Phase Lag..... 72
6.5.3	Modeling..... 73
CHAPTER 7	<u>CONCLUSIONS AND RECOMMENDATIONS</u> 76
REFERENCES 78
APPENDICES
APPENDIX I	INPUT SINE WAVE CHARACTERISTICS..... 81
APPENDIX II	EXPERIMENTAL DATA..... 86
APPENDIX III	OUTPUT SINE WAVE CHARACTERISTICS..... 93
APPENDIX IV	FLUOROMETER AND KINETIC CLAMP PUMP CALIBRATION CURVES..... 102
APPENDIX V	MODELING..... 108

LIST OF FIGURES

<u>FIGURE</u>	<u>DESCRIPTION</u>	<u>PAGE</u>
1	INPUT-OUTPUT SINE WAVE RELATIONSHIP	19
2	BODE PLOT OF RESPONSE FROM AN IDEAL CSTR	26
3	DIAGRAM OF EXPERIMENTAL EQUIPMENT	31
4	TEST VESSEL CONFIGURATIONS	46
5A	DATA FROM EXPERIMENTS I AND II -	48
5B	NO MIXING PROVIDED	49
6A	MODEL PREDICTIONS FOR EXPERIMENT I	53
6B	VESSEL A - NO MIXING PROVIDED	54
7A	MODEL PREDICTIONS FOR EXPERIMENT II	56
7B	VESSEL A - NO MIXING PROVIDED	57
8A	DATA FROM EXPERIMENTS I AND II -	59
8B	MIXING PROVIDED	60
9A	MODEL PREDICTIONS FOR EXPERIMENT I	62
9B	VESSEL A - MIXING PROVIDED	63
10A	MODEL PREDICTIONS FOR EXPERIMENT II	64
10B	VESSEL A - MIXING PROVIDED	65
11A	DATA FROM EXPERIMENT III -	67
11B	NO MIXING PROVIDED	68
12A	MODEL PREDICTIONS FOR EXPERIMENT III	70
12B	VESSEL B - NO MIXING PROVIDED	71
13	SCHEMATIC OF SINE WAVE GENERATING APPARATUS	82
14	TYPICAL INPUT AND OUTPUT SINE WAVES	96
15	FLUOROMETER CALIBRATION CURVE A	103
16	FLUOROMETER CALIBRATION CURVE B	104
17	FLUOROMETER CALIBRATION CURVE C	105
18	FLUOROMETER CALIBRATION CURVE D	106
19	KINETIC CLAMP PUMP CALIBRATION CURVE	107

LIST OF TABLES

<u>TABLE</u>	<u>DESCRIPTION</u>	<u>PAGE</u>
I-1	COMPARISON OF INPUT SIGNAL TO SINE FUNCTION	84
II-1	DATA - EXPERIMENT I - NO MIXING PROVIDED	87
II-2	DATA - EXPERIMENT I - MIXING PROVIDED	88
II-3	DATA - EXPERIMENT II - NO MIXING PROVIDED	89
II-4	DATA - EXPERIMENT II - MIXING PROVIDED	90
II-5	DATA - EXPERIMENT III - NO MIXING PROVIDED	91
II-6	DATA - EXPERIMENT IV - NO MIXING PROVIDED	92
COMPARISON OF OUTPUT SIGNALS TO SINE FUNCTION		
III-1	EXPERIMENT I TEST II RUN B	94
III-2	EXPERIMENT I TEST I RUN C	95
III-3	EXPERIMENT II TEST I RUN D	97
III-4	EXPERIMENT II TEST II RUN D	98
III-5	EXPERIMENT III TEST I RUN A	99
III-6	EXPERIMENT III TEST I RUN C	100
III-7	EXPERIMENT IV TEST I RUN E	101
MODELING		
V-1	EXPERIMENT I - NO MIXING PROVIDED	109
V-2	EXPERIMENT I - NO MIXING PROVIDED	110
V-3	EXPERIMENT II - NO MIXING PROVIDED	111
V-4	EXPERIMENT II - NO MIXING PROVIDED	112
V-5	EXPERIMENT I - MIXING PROVIDED	113

<u>TABLE</u>	<u>DESCRIPTION</u>	<u>PAGE</u>
V-6	EXPERIMENT I - MIXING PROVIDED	114
V-7	EXPERIMENT II - MIXING PROVIDED	115
V-8	EXPERIMENT II - MIXING PROVIDED	116
V-9	EXPERIMENT III - NO MIXING PROVIDED	117

CHAPTER 1

INTRODUCTION

1.1 Purpose and Scope of the Investigation

In the field of Sanitary Engineering, many types of water and waste treatment facilities incorporate some type of reaction vessel to carry out the purification or treatment process. In most cases the reaction vessels are designed to conform to conventional, empirically derived, design criteria and as such, these reactors can be expected to embody something less than ideal fluid flow properties.

To better understand and describe the reactions which take place in non-ideal flow vessels, a method is needed to measure and evaluate the hydraulic characteristics or fluid flow properties of these vessels. The method chosen should, ideally, be an accurate and easily applied technique to measure system response. Further, to aid in the prediction of system response under varying conditions, it would be advantageous to be able to describe the vessel's behavior in terms of well known and easily defined ideal components or reactors.

The frequency response technique is a method of analysing, testing, and controlling various networks and systems. This technique was first applied in the Electrical Engineering field of servomechanisms and has since become a useful and widely accepted technique in that field. As well, the frequency response technique has been successfully applied in

Chemical Engineering process control work. However, to date, there has been very little study or research done to investigate the potential of applying this technique to Sanitary Engineering systems.

The purpose of this research project is, therefore, to explore the feasibility of adapting this technique to analyse and describe reaction vessels commonly utilized in water and waste treatment processes.

To successfully apply this method of analysis, it initially had to be proven that specific cyclic disturbances could indeed be successfully produced and monitored. This involved construction and testing of several types of apparatus before suitable equipment was developed and refined to a point where data could be gathered. The data then had to be evaluated to determine if it was meaningful and whether it could be represented utilizing methods commonly employed in frequency response analyses.

Based on the experimental data, the next and final stage in the study was to investigate the feasibility of modeling conditions in the test reactor by means of a simple network of ideal, mathematically describable, components.

1.2 Possible Applications of this Work

To successfully describe and predict the conversion in a continuous reactor, both the kinetics of the reaction involved, and the hydraulic characteristics of the reaction

vessel must be known. If only the reaction kinetics are known, then by measuring the conversion that takes place, some insight can be gained into the fluid flow properties of the vessel. Conversely, if the hydraulic characteristics of the vessel are known, an understanding of the reaction kinetics involved can be gained by studying the properties of the effluent produced.

Unfortunately in many waste treatment applications neither the reaction kinetics nor the hydraulic characteristics of the reaction vessel are completely understood. This lack of basic information has resulted in the use of empirical design standards or "rules-of-thumb". These design criteria are based on observed performance of various, often unrelated facilities, and as such are relatively inflexible in that they cannot be tailored to meet the requirements of a specific waste or a specific degree of treatment.

It is therefore evident that a more rational approach is needed both to evaluate and describe the performance of existing waste treatment facilities and to develop and refine design practices to optimize process efficiency. The frequency response technique shows promise of being a method of analysis well suited to the accurate measurement and description of the hydraulic characteristics or fluid flow properties of waste treatment reaction vessels.

If application of this technique proves to be feasible,

it could be used to investigate and analyse the performance of many types of commonly used waste treatment processes. One such application could be in studying the performance of aeration tanks, which are the core of the widely used "activated sludge process" and modifications thereof. Several theories or opinions have been voiced as to the actual working characteristics of such reactors and as to how installations should be designed to provide optimum treatment. These opinions have, at one extreme, described aeration tanks as plug flow vessels while others maintain that completely mixed conditions exist in the reactor. By applying frequency response analysis, it should be possible to accurately measure the system response from aeration tanks and describe this response in terms of ideal fluid flow vessels. This measurement and description of system response would make possible both the development of more refined design practices and the prediction of what changes are necessary to optimize process efficiency of existing installations.

Partially mixed treatment systems such as oxidation ditches or aerated waste stabilization ponds could also benefit from frequency response analysis. By application of this technique to measure the response from existing reactors, it should be possible to describe the mixing characteristics in terms of percentage of reactor volume which is completely mixed, percentage which is dead space etc. Such a model or

description would give an insight into the reactions taking place in the vessel and further, provide a basis to evaluate the effectiveness of design alterations.

A third major application for frequency response techniques could be in the field of stream or river assimilation studies. By injecting cyclic disturbances of a tracer into a stream and analysing the response, it should be possible to model the stream with a system of ideal components which produce an identical response when forced in the same manner. Since the reaction behavior of the ideal components in the model are all defined mathematically, it would be possible to predict the conversion which would occur if a waste with known reaction kinetics were introduced into the stream. In this way, stream assimilation capacity and downstream quality of a body of water could be easily and accurately predicted.

CHAPTER 2

REVIEW OF RELATED WORK

2.1 General Statement

The problem of adequately measuring and describing the flow characteristics of reactors used in sanitary engineering treatment processes is not a new one. A great deal of research has been carried out to try and resolve this problem. To a large extent, this research work has centred around the investigation of the aeration tank of the activated sludge process, since this is one of the most popular methods of waste treatment. The following brief reference to past work in the field is therefore concerned mainly with aeration tanks. However this review is useful in that it is indicative of the general techniques and methods of analysis which have been used to date.

2.2 Methods of Analysis

The first attempt to quantitatively analyse aeration tanks was carried out by Kessner (12) when he used a unit pulse of salt or chloride tracer in a three cell aeration tank to determine if short circuiting were occurring. By observing the resulting concentrations of salt throughout the three cells he was able to conclude that no hydraulic short-circuiting was occurring but that mixing or "relative short-circuiting" was an important parameter. Today Kessner's "relative short-circuiting" mechanism is recognized as turbulent dispersion.

This work was followed by Kehr (11) who introduced a step function of chloride to a longitudinally halved experimental aeration tank. Comparison of the test data to a basic equation relating concentration and time in a mixed tank subjected to a step function disturbance enabled Kehr to conclude that one compartment of the experimental tank approached perfect mixing while an "around the end" arrangement using the other half of the tank in series approximated two perfectly mixed tanks in series.

The next tracer oriented work of significance was by (33) Thomas and McKee who carried out extensive studies to define longitudinal mixing in aeration tanks. A pulse input of chloride was used with water as the carrier liquid. The concentration of salt in the test media was determined both by conductivity measurements and titration techniques. The end result of this work was the development of an equation which relates pulse induced tracer concentration to time and distance along a closed vessel. By varying the value of a turbulent expression in this equation good correlation was achieved between the theoretical curve and experimental pulse tracer outputs. The experimental data was also fitted with a model consisting of a number of perfectly mixed tanks in series. It was noted that an increase in the number of mixed tanks produced a decrease in the degree of longitudinal mixing.

More recently, research has been done in the Chemical

Engineering field to define the flow characteristics and dispersion in chemical reactors. The dispersed plug flow model has been developed as a result of work done by Danckwerts (6), Levenspiel (16, 18) and others. The basic assumption in the development of the dispersed plug flow model is an equation similar to Fick's second law for molecular diffusion. By analysing experimental results for variance and relating this to a dispersion coefficient, a fit between the experimental findings and the predicted response from the dispersed plug flow model can be achieved.

Aside from this, Pipes et.al (28, 29) have suggested that a number of equal-volume perfectly mixed tanks-in-series could be used for modeling purposes or that a mixed model consisting of various combinations of complete mixing, plug flow, short-circuiting, stagnant zones, and recycle might serve to represent the hydraulic characteristics of mixing tanks. However, both the tank-in-series, and the dispersion model have been questioned and Levenspiel (17) states that these models are unsuitable

when the gross flow pattern deviates greatly from plug flow because of channeling or recirculation of fluid, eddies in the odd corners, etc.

Timpany's (32) study of variations of axial mixing in aeration tanks would seem to refute this last statement. Timpany found that the dispersed plug flow model can adequately describe the longitudinal mixing conditions in highly

mixed spiral flow aeration tanks. This conclusion was reached using pulse tracer inputs of Rhodamine B in both a laboratory scale aeration tank and a full scale aeration tank.

In summary, a somewhat confused picture is presented as to how mixing tanks can best be described. Various researchers have developed several different models to describe the hydraulic patterns of mixing tanks. First, plug flow was assumed, then a more accurate insight was gained using ideal mixing. Next, a dispersed plug flow model, then a tank-in-series model, and finally a mixed model were described as being representative.

2.3 Discussion

Although these examples of tracer techniques and modeling procedures are only indirectly related to the topic of this thesis, it was felt that a brief survey of background information in this field was necessary to effectively point out the need for a more generalized and flexible approach to the problem of accurately describing the hydraulic characteristics of reaction vessels.

The major part of this work has followed a fairly well defined pattern -- that is in each case an attempt was made to arrive at a single equation which would completely describe the flow-through characteristics of the vessel under study. To do this, researchers have first postulated a theoretical model or equation and then have employed some type

of transient tracer technique to gather data. The data was then used to verify the assumed model and to adjust parameters in the postulated equation so that a close theoretical to experimental correlation could be achieved.

This method of approaching the problem has merit and there is no doubt that under certain conditions, each model can adequately describe a specific system or reactor. However there are shortcomings involved in the one equation approach in that once the equation has been postulated, the subsequent experimental proof is restricted in nature to conform to the limitations imposed by the assumed model.

It would seem that there is no need to initially develop an equation to describe a system, but rather it should be possible to use experimental findings to develop a model consisting of a network of basic ideal components which would respond identically when forced in the same manner. Such ideal components as perfectly mixed tanks, plug flow reactors, dead space, etc. could be used in the modeling network. Since all of these ideal components are well defined mathematically, their reaction to any forcing function can easily be found and it should then be possible to build a network that would respond in the required manner. The only assumption required in this approach is that the test system can be described either by a CSTR or a PFTR or by some arbitrary network combination of the two. Using just these two ideal

components, an infinite variety of networks can conceivably be postulated to predict the response from a partially mixed test system. Model development is therefore very flexible. No initial assumption is necessary as to how the system should react so that modeling is not limited to the confines of a specific preselected equation. An added benefit would be that any such model could be easily understood since the basic components are all well defined and commonly encountered in the sanitary engineering field.

The first step then, in describing a system in this manner, would be to gather reliable data from the system under study. To do this, an accurate tracer technique is required. For ease of modelling the tracer technique chosen should produce a predictable, well defined output from the basic components which are to make up the model. Any of the transient tracer techniques previously mentioned, such as delta, step or ramp functions, fit this criteria to some extent in that their theoretical output from a given ideal component is well known. However, in application to a real system these forcing techniques vary somewhat from their theoretically assumed properties. For example, the pulse or delta function is theoretically described as a disturbance of infinite magnitude and zero time duration. Physically, such a disturbance is impossible to create. The same is true of step or ramp functions which are idealizations that can

never be exactly created physically. (27) This shortcoming may be a matter of little importance when the duration and magnitude of the disturbance is much smaller than the time constants of the system under study, but this limitation does detract from using transient techniques in that some restrictions have been placed on the type of system that can be studied using this technique.

Another property of transient tracer techniques is that in most cases, the response to any type of discontinuous forcing function bears little if any resemblance to the input function. (27) For example the response to a step function introduced into a CSTR is not a step function but rather an exponential function. In modeling on the one equation approach, this would not be a limiting factor since the output from one component is all that is required. However, in this study, where it is proposed to model using networks of ideal components, it is possible that several components in series or in parallel would be required to adequately describe a system. In this case the output from the first component would become the input to the second component, the output from the second would become the input to the third, etc. In this regard, Harriott (9) has commented that:

....calculations of the transient response are quite tedious with only three components in the system and are too difficult to be worthwhile for four or more components.

From the foregoing it can be appreciated that transient tracer techniques have several undesirable qualities which limit their usefulness as analytical or experimental techniques. By contrast, frequency response analysis of a system or component avoids many of the limitations imposed by transient techniques and offers several advantages. Frequency response is a technique that was developed within the field of servomechanisms and has since been found to have a very direct application in any area of automatic-control analysis. This technique is both an experimental and analytical tool consisting of a study of the response of components or systems to sinusoidal inputs of different frequencies. (20)

The popularity and widespread use of this technique in electrical engineering and process control work stems from basic inherent qualities of the sine wave. The sine wave is the only periodic signal which maintains its waveform when it is differentiated, integrated, or multiplied by a constant. This is important when it is realized that any linear system operates on signals in such a way that they are differentiated, integrated or multiplied by a constant. Thus, a sinusoidal waveform can pass through a linear system with its basic characteristics intact and emerge as a sinusoidal waveform. This is not true of any other periodic function and the only aperiodic or transient signal which has this property is the exponential function. (19) This property lends itself well

to a multi-component modeling procedure. With transient response techniques there is no continuity in input characteristics from one component to another in a series. However, with frequency-response analysis, the output from one component and therefore the input to the next component in a series, will retain the basic sinusoidal characteristics of the original input function. This fact should simplify multi-component analyses and avoid some of the difficulties in calculation which are associated with transient tracer techniques.

Another important property is that the sum of two sine waves of equal period is also a sine wave. It is therefore possible to take two sine waves with arbitrarily chosen amplitudes and initial phase angles, and, provided the periods are the same, the two waves can be added to form a sinusoidal wave. This can, of course, be extended to include any number of sinusoidal components of equal period.

A third useful characteristic of the frequency response technique is the fact that only the steady state portion of the sinusoidal response curve is of value in analysing a system. (21) Therefore any initial transient behavior can be disregarded and so the effects of initial conditions need not be taken into account.

The use of this technique is well documented in both electrical engineering and chemical process control and many

textbooks such as those by Harriott, (9), Murrill, (20), Coughanowr and Koppel, (5), Perlmutter, (27), Lynch and Truxal, (19), etc. have been published which give evidence that frequency response is a "potent and widely accepted tool for the analysis of control systems." As well, Murrill (21) stated that frequency response is useful:

1. For the analysis, synthesis, design and compensation of systems or components.
2. For the experimental determination of characteristics and working equations to describe systems without relying entirely on a theoretical derivation of the analytic equation.

2.4 Frequency Response References

To date, very little work has been done to determine if this technique could be beneficially applied to systems and components commonly used in environmental engineering work. In fact, actual experimental use of the frequency response technique has not been widespread as the major portion of its application has been limited to "the pencil and paper study of control systems or components". (20)

In 1953, in Chemical Engineering Progress, Wilhelm (34) illustrated that the frequency response technique could be physically applied to study diffusion in packed beds. This technique was used since it was realized that while passing a single concentration or temperature pulse through a bed is very simple experimentally, it produces mathematically complex results. Using gas as a tracer, it was found that

axial diffusion between particles and diffusion within particles could be measured by studying the decrease in amplitude and shift in phase angle of the sinusoidal function as it was acted upon by diffusion mechanisms within the bed. The researchers concluded from this work that frequency-response was a useful experimental procedure and offered the advantage of allowing simultaneous investigation of several processes or components so that the final piece of industrial type equipment could be investigated in place.

Similarly, Kramers and Alberda (13) experimentally applied the frequency response technique to investigate the dispersion model. It was found that the phase lag and attenuation of a sinusoidal input signal as it passed through a vessel yielded the desired information concerning the dispersion coefficient.

Lee and Hougen (15) used frequency response analysis to investigate a steam-jacket heat exchange. A sinusoidal variation in pressure was applied to the outlet control-valve stem, thus causing a similar variation in the flow of water through the exchanger. Steam pressure and inlet water temperature were maintained constant. The effluent water temperature and valve stem position, both varying sinusoidally were recorded as functions of time. By testing the system over a range of frequencies sufficient data was gathered to accurately correlate valve stem position and effluent tempera-

ture.

Geerlings and Kramers (8) used frequency response testing to study the sodium hydroxide-carbon dioxide neutralization in a continuous flow, pilot size apparatus. Mechanical agitation was used to intimately mix pure carbon dioxide feed with the liquid. The pure gas was introduced at a sinusoidally varying rate and the solute concentration in the effluent liquid was continuously monitored. The frequency response data gathered in this way was used to develop a first-order transfer function which successfully modeled the experimental findings.

A considerable amount of actual physical testing with frequency response techniques has been done in evaluating the control of pH and blending processes. In this work, the "mixing delay" or the time required to realize a change in feed concentration is often the second largest lag and thus has a large influence on the system performance. Kramers (14) was the first to use frequency response tests to determine the mixing delay for a continuous-flow stirred tank. By monitoring the exit pH while the system was sinusoidally forced, the mixing delay was accurately calculated. In a similar study, Colucci (4) determined mixing delays for a 3 foot baffled tank with a flat paddle stirrer. As well, it was found that the mixing delay varies inversely with a fractional power of the stirrer speed and decreases with

decreasing gross fluid residence time.

In addition to the relatively few times that frequency response testing has actually been physically applied, several authors, (3), (10), (31) have developed techniques for converting transient data into frequency response data. These techniques in general require a great amount of computational effort and are best suited to reduction on a digital computer. In this vein, Adler (1) and Rooze (30) have developed a numerical technique to transform residence time distribution information to the s-plane. From the transformed information a particular model consisting of a number of stages was developed to represent the fluid flow characteristics of any reactor. Each stage of the postulated model is made up of a pair of equal volume CSTR's linked in parallel.

In summary, this review of work done with frequency response analysis indicates that this technique has been successfully applied to investigate the properties of a wide variety of systems ranging from a heat exchanger to a catalytic bed. It therefore appears feasible to use this testing method to gather data to characterize reaction vessels such as are commonly used in water and waste treatment processes.

CHAPTER 3

THE CONCEPT OF FREQUENCY RESPONSE3.1 Theory

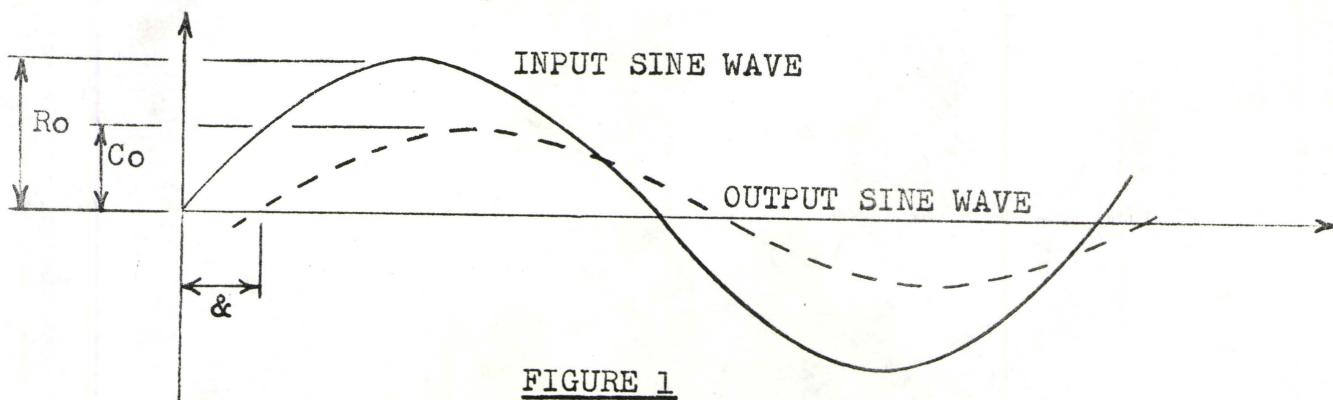
The underlying principle involved in utilizing the frequency response technique is that:

when a stable linear system is forced sinusoidally, it shows transient behavior for a limited time depending on initial conditions, and then it responds sinusoidally.

(27)

This property, as indicated previously, arises from the fact that linear systems alter a signal by differentiation, integration, multiplication by a constant, or by a linear combination of these operations, and since a sine wave maintains its waveform throughout these operations, then the steady-state system response must also be sinusoidal.

Although a sinusoidal forcing function passes through all linear operations with its basic characteristics intact, the wave does change in dimension and position on the time axis. (27) The changes in dimension and position provide valuable information on the system involved and form the raw data with which frequency response studies can be made. These properties can be best understood and explained by means of a diagram such as is shown in Figure 1.



In this diagram the excitation or variation in the input variable to the component or system is a sine wave of amplitude R_o and frequency w . For a linear system, the output response or variation in the output variable will be another sine wave of amplitude C_o and of the same frequency as the input wave. However, the output wave will be displaced from the input wave by a phase angle " ϕ ". Frequency response analysis is based on studies of the variation in the amplitude ratio C_o/R_o for various values of the frequency of the input wave w , and on studies of the variation in the phase angle " ϕ " for various values of w .

3.2 Linearity and Stability

The restriction placed on the use of frequency response analysis is that it is applicable only to stable time invariant linear systems. By a linear system it is meant that the system can be described by a differential equation in which no terms exist of degree greater than one in the dependent variable. The stability criteria is satisfied if all of the roots of the characteristic equation have negative real parts.

An example of a linear system would be a CSTR which has a constant volume as well as equal and constant rates of input and output. Such a reactor can be described by the differential equation:

$$Vdy/dt = qx - qy \quad \dots\dots(1)$$

where V = reactor volume
 x = input concentration
 y = output concentration
 q = flow rate
 t = time

This is a linear differential equation in which there are no terms of the dependent variable, y , greater than one. Also the coefficients, in this case q and V , are constant and independent of time. If the flow rate were to vary with time this would still be a linear system but could not be analysed using frequency response methods since the coefficients of the equation would not be constant.

The restricted application of frequency response analysis to only stable time invariant linear systems should pose no problem with regard to modeling since it can be shown that both a CSTR and a PFTR, to be used in the modeling network, are linear in nature. Also, since during the experimental phase of this work flow rate and reactor volume were kept constant over a range of frequencies, no problems should be encountered with non-constant coefficients. Knowing this, in order to apply frequency response analysis to this work, it would remain to be proven that the actual test vessel could be described by a linear differential equation with constant coefficients. This was **not** done directly but can be partially shown by the fact that the actual output from the experimental system was definitely sinusoidal in nature (Appendix III). The experimental system, therefore, satisfied the criteria that a stable linear system, when forced sinusoidally, will respond in a sinusoidal manner.

3.2 Data Analysis and Representation

Frequency response analysis of a system or component is basically a study of the amplitude attenuation and phase shift which result when a sine wave is passed through the system. To theoretically predict the response of any system to a sinusoidal input, it is therefore necessary to calculate the system output with time. Such calculations can become time consuming and tedious especially as the differential equation describing the system becomes more complex. To avoid these computational difficulties, to some extent, it has become common practice to use Laplace transforms which can be defined as:

$$F(s) \equiv \mathcal{L}[f(t)] \equiv \int_0^{\infty} f(t)e^{-st} dt$$

where $f(t)$ represents a time function
 $F(s)$ is a function of the complex variables
 (Note: s must be chosen so that convergence of this improper integral is guaranteed)
 \mathcal{L} denotes the transform process

By using this transform a differential equation can be reduced to an algebraic equation with the complex variable s replacing time as the independent variable. The algebraic equation can then be solved and returned to the time domain by means of an inverse transform.

This procedure can be illustrated by using Equation (1)

$$V/q \, dy/dt = x - y$$

$$\text{or } dy/dt + y = x \quad \dots\dots(2)$$

which is the linear differential equation describing a well

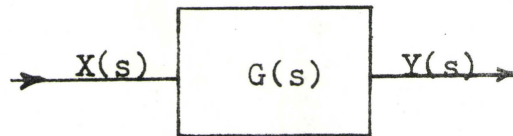
mixed vessel. When transformed this equation becomes:

$$\tau s Y(s) + Y(s) = X(s) \quad \text{assuming } Y(0) = 0$$

$$\text{or } Y(s) = X(s) (1/(\tau s + 1)) \quad \dots\dots(3)$$

$$\text{or } Y(s) = X(s)G(s) \quad \dots\dots(4)$$

where $G(s) = 1/(\tau s + 1)$ is defined as the system or transfer function. Equation (4) can be shown in block-diagram notation as:



Now if the input concentration is forced sinusoidally by the function $x(t) = a \sin wt$ or when transformed

$$X(s) = aw/(s^2 + w^2)$$

$$\text{then } Y(s) = G(s)X(s) = aw/(s^2 + w^2) G(s) \quad \dots\dots(5)$$

When this is expanded by partial fractions

$$Y(s) = (K_1 w + K_2 s)/(s^2 + w^2) + K_3/(s + \lambda_3) + K_4/(s + \lambda_4) + \dots\dots(6)$$

where: $\lambda_3, \lambda_4 \dots$ are the poles of the transfer function $G(s)$

If the inverse transform of this is taken the system output is found to be:

$$y(t) = K_1 \sin wt + K_2 \cos wt + K_3 e^{-\lambda_3 t} + K_4 e^{-\lambda_4 t} \dots$$

$$\text{or } y(t) = K \sin(wt + \phi) + K_3 e^{-\lambda_3 t} + K_4 e^{-\lambda_4 t} + \dots\dots(7)$$

It is evident from equation (7) that the exponential terms must represent the transient behavior of the system which will die out as t becomes large, if λ_3, λ_4 have positive real parts, thus leaving the sinusoid as the only time varying function.

Also looking at the terms K and ϕ in equation (7) it becomes

evident that K represents the output wave amplitude while ϕ represents the phase lag.

To evaluate K and ϕ (or what amounts to the same K_1 & K_2) equation (6) is multiplied by $(s^2 + w^2)$ to yield:

$$aWG(s) = K_1 w + K_2 s + (s^2 + w^2)K_3 / (s + \lambda_3) + \dots (8)$$

Now evaluating this expression when $(s^2 + w^2) = 0$ or when $s = jw$ it is found that:

$$G(jw) = \frac{K_1}{a} + \frac{K_2 j}{a} \dots (9)$$

If the particular transfer function $G(s) = \frac{1}{\tau s + 1}$, representing a well mixed tank, is treated in this manner it gives $G(jw) = \frac{1}{1 + \tau(jw)}$, or by rationalizing the denominator:

$$G(jw) = \frac{1}{1 + w^2 \tau^2} - \frac{w\tau}{1 + w^2 \tau^2} j \dots (10)$$

by comparison with equation (9), it can be seen that the term

$$\frac{K_1}{a} \text{ corresponds to } \frac{1}{1 + w^2 \tau^2}$$

$$\text{and } \frac{K_2}{a} \text{ corresponds to } - \frac{w\tau}{1 + w^2 \tau^2}$$

If equation (9) were plotted as a vector in the complex plane, then,

$$\text{magnitude} = |G(jw)| = \frac{\sqrt{K_1^2 + K_2^2}}{a}$$

$$\text{and angle} = \angle G(jw) = \arctan \left(\frac{K_2}{K_1} \right)$$

Similarly for equation (10)

$$|G(jw)| = \frac{1}{(1 + w^2 \tau^2)^{1/2}}$$

and $\angle G(j\omega) = -\arctan \omega\tau$

By inspection it becomes evident that the output amplitude is smaller than the input by a factor $\left\{ \frac{1}{(1+\omega^2\tau^2)^{1/2}} \right\}$ and is delayed by the phase angle $\phi = -\arctan \omega\tau$. It is also apparent that if τ (or really V and q) is kept constant, then output amplitude and phase lag are only functions of frequency ω .

This example serves to point out the fact that the transfer or system function is a fundamental way of describing the dynamic properties of a linear system. Linear system analysis is, to a large extent, built around the transfer function and it is frequently possible to deduce important characteristics of system response merely by inspection of the nature of the various terms comprising the transfer function. (19) Also, from a practical viewpoint, the derivation and exact meaning of the Laplace transform need not be understood but rather it can be used just as a computational tool (9).

It has been seen that the systems effect on amplitude and phase angle is a function of the frequency ω . A convenient graphical representation of the dependence of these two parameters on frequency was developed by H.W. Bode (2) who did a great amount of early work in the field of servomechanisms. The Bode plot which has received very widespread acceptance consists of a set of two graphs which show the

variation of amplitude ratio ($|G(j\omega)|$) and phase lag ($\angle G(j\omega)$) with frequency. One graph shows the logarithm of amplitude ratio as plotted against the logarithm of frequency while on the second graph the phase angle versus the logarithm of frequency is plotted.

A typical Bode plot for the well mixed vessel example can be represented as in Figure 2. (9)

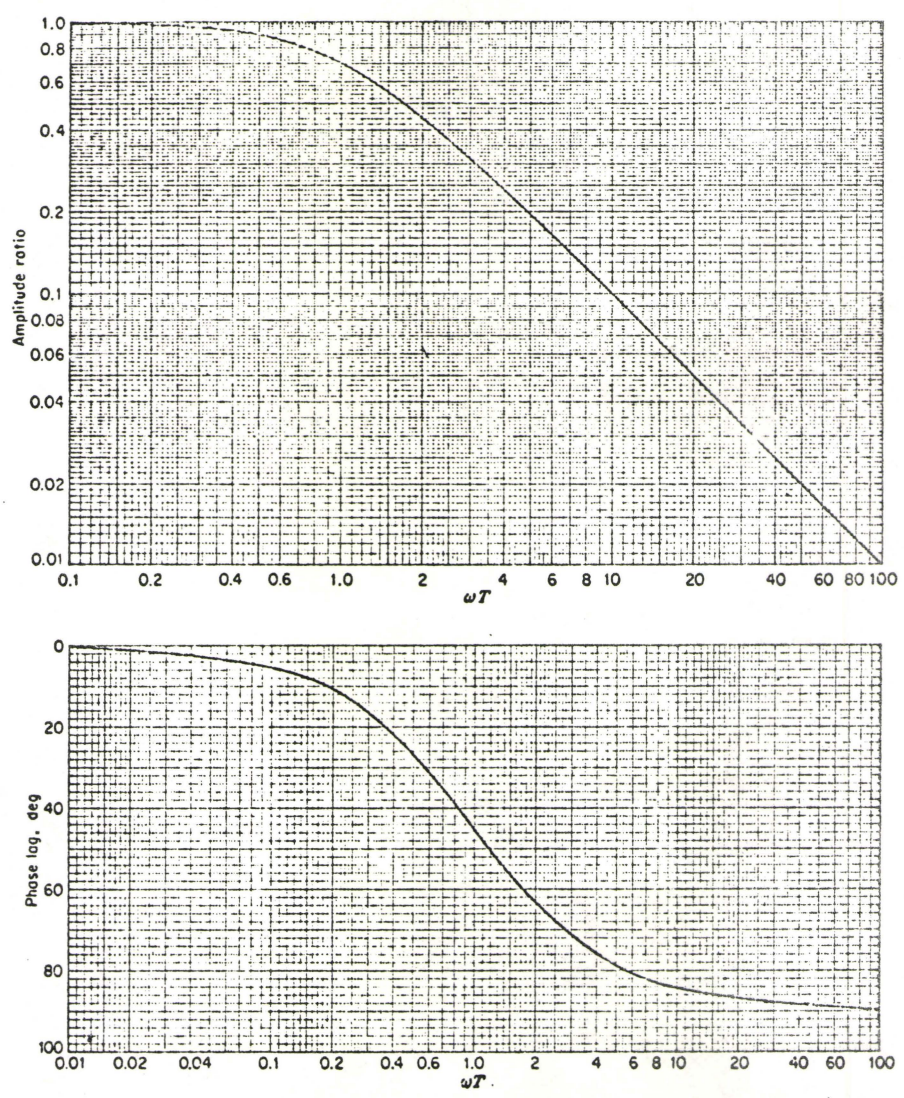


FIGURE 2

On inspection, this diagram illustrates a facet of Bode plots which makes their construction much simpler and more useful. The log magnitude plot is very closely approximated by two asymptotes, one for low frequencies and one for high frequencies. (20) To find the asymptotes, it is necessary to consider that as the frequency becomes very small, or conversely as the period increases

$$\lim_{w \rightarrow 0} |G(jw)| = \lim_{w \rightarrow 0} \frac{1}{(1+w^2\tau^2)^{1/2}} = 1$$

this is the low frequency asymptote, which in log scale is represented by a line of slope 0.

Also since

$$\begin{aligned} \lim_{w \rightarrow \infty} \log |G(jw)| &= \lim_{w \rightarrow \infty} (-\log \sqrt{1+w^2\tau^2}) = -\log w\tau \\ &= \log w - \log \tau \end{aligned}$$

Therefore for each tenfold increase in w , there will be a -1 change in $\log |G(jw)|$ so that the curve approaches a straight line of slope = -1.

The low frequency and high frequency asymptotes with slopes of 0 and -1 respectively intersect where $w = 1/\tau$ which is called the corner frequency.

By treating the phase lag curve in a similar manner, it can be shown that

$$\lim_{w \rightarrow 0} \angle G(jw) = \lim_{w \rightarrow 0} \arctan (-w\tau) = 0^\circ$$

$$\text{and } \lim_{w \rightarrow \infty} \angle G(jw) = \lim_{w \rightarrow \infty} \arctan (-w\tau) = -90^\circ$$

Also at the corner frequency where $\omega = 1/\tau$

$$\angle G(j\omega) = \arctan(-1) = -45^\circ$$

Another advantage of utilizing a Bode plot for data presentation and modeling purposes becomes evident when considering a number of systems or elements in a series. Since the overall transfer function of a system composed of several elements is simply the product of the individual transfer functions for each element, then the overall amplitude ratio can be found by multiplying the individual amplitude ratios. Similarly, the system phase lag is obtained by adding all of the individual lags of each component. The overall system response is therefore independent of the order of the various elements in the system. This property arises from the rules for multiplication of complex numbers. The real parts of the numbers which represent the amplitude ratios can be multiplied while the imaginary parts, representing the phase angles, are added.

Since, on a Bode plot, amplitude ratios are plotted in logarithmic scale, then several amplitude ratios can be combined merely by graphically adding the distances from the line where amplitude ratio equals one. This greatly simplifies analysis of multi-component systems. Rather than multiplying all the individual transfer functions and algebraically solving an unwieldy equation, it is often simpler to show the Bode plot for each element and arrive

at an overall Bode plot by graphical means. Since, in essence, the Bode plot of each individual element represents the transfer function of that element, then the composite Bode plot is equivalent to the total system transfer function.

The ability to graphically analyze a system is of particular importance when modeling. Bode plots for ideal components such as C.S.T.R.'s, P.F.T.R's, by-pass and dead space can be plotted individually and then a composite plot arrived at which corresponds to the experimentally obtained Bode plot. In this way, it is not necessary to deal with complex differential equations or Laplace transforms until the correct model has been found and even then little purpose may be served in describing the model in terms of a single equation.

CHAPTER 4

EXPERIMENTAL METHOD4.1 Experimental Equipment

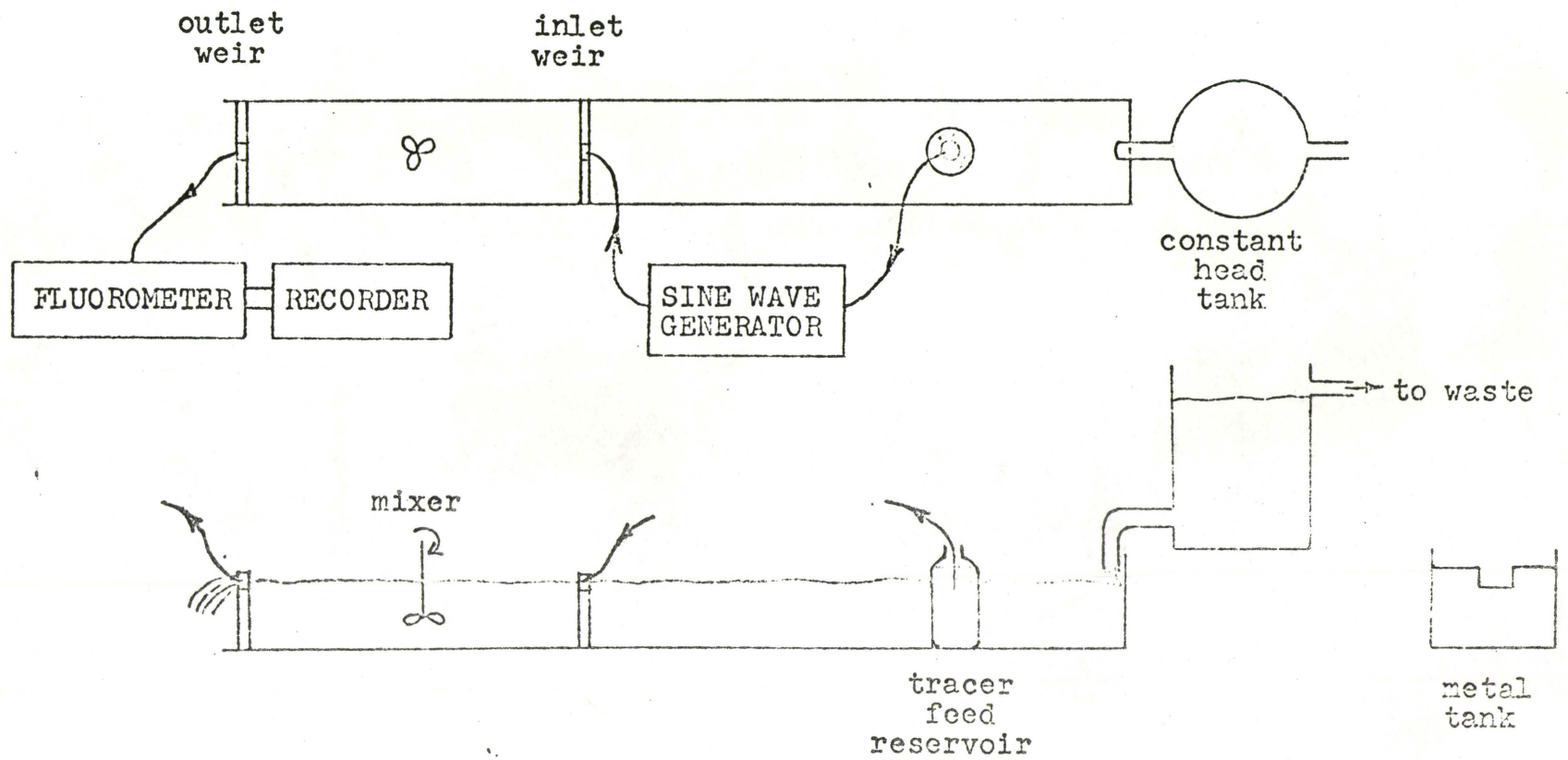
A flow through vessel of arbitrary configuration was used in this study. It consisted of a rectangular metal tank as shown in Figure (3). The weir at the discharge end of the vessel was fixed in position while the influent weir was moveable so that the length of the vessel could be altered and thereby at a constant flow rate, fluid residence times and hydraulic characteristics could be varied.

The liquid used in the flow through reactor was Hamilton tap water. The flow rate could be varied so that any tank configuration could be investigated over a range of fluid residence times. During any specific test run, the flow rate was regulated by means of a constant head tank with the actual flow being measured using a volumetrically calibrated 2.5 litre container. Although no attempt was made to maintain the test liquid at a constant temperature, continuous monitoring with a Tele-Thermometer produced by the Yellow Springs Instrument Company revealed that temperature was a near constant at 19 degrees centigrade.

The apparatus used to generate a sinusoidally varying flow of tracer consisted of a 1/6 H.P. Westinghouse A.C. motor (1725 RPM) coupled to a Zero-Max model 142-X variable speed torque convertor manufactured by the Revco Corporation. A 1-5/8 inch diameter V-belt pulley on the output shaft of

FIGURE 3

DIAGRAM OF EXPERIMENTAL EQUIPMENT



the gear reducer drove a 12 inch diameter V-belt pulley mounted on a horizontal shaft. Fixed to the end of the horizontal shaft was a $1\frac{1}{2}$ inch long acrylic plastic arm pin connected to an acrylic plastic driving rod ten inches in length. This driving rod was in turn pin connected to a length of brass gear rack which was restricted in movement to the horizontal plane by two plastic runner guides. The rack engaged a brass spur gear connected to a circular rheostat which varied the current supplied to a D.C. motor internally contained in a Sigmamotor variable flow kinetic clamp pump. The reciprocating motion of the gear rack alternately increased and decreased the pump motor speed, thereby producing a sinusoidal flow of tracer. A schematic diagram of this signal generating and the mathematical proof that this assembly produced a sine wave is contained in Appendix 1.

The frequency of sine wave generation was controlled by altering the reduction ratio of the variable speed gear reducer. It was found that sine waves with approximate maximum and minimum periods of 8 minutes and 30 seconds respectively could be reliably produced. At frequencies lower than $1/480$ cycles per second (period of 8 minutes) the gear reducer tended to slip and produce distorted sine waves. The exact period of each sine wave used in the experiment was measured on the effluent recording chart and cross-checked by timing revolutions of the drive pulley. Also, although it was not

done in this study, the amplitude of the sine wave produced could be increased or decreased by using a smaller or a larger spur gear respectively.

The kinetic clamp pump feeding the tracer was calibrated to determine if fluid flow varied linearly with rheostat settings from zero flow to one hundred percent flow. The relationship between milliliters of fluid pumped and rheostat setting was found to have a linear relationship between 10% and 90 % maximum flow. The variations in flow from 20% to 80% as used in the experimental tests were therefore well within the linear portion of the calibration curve for this pump.

For this type of tracer study on a continuous flow system a tracer is required which is miscible with the carrier fluid, not naturally present in the carrier fluid, is not created or destroyed by reaction and is not readily absorbed or adsorbed by any of the constituents present in the carrier fluid or by any of the materials in the vessel under study. The tracer used in this work was Rhodamine Lissamine B-200 (colour index - 45100). The acceptability of this tracer has been documented by Feuerstein and Selleck (7) in a study which compared the behavior of fluorescent tracers Rhodamine B, Pontacyl Brilliant Pink B, and Fluorescien in waters of various qualities. Although Rhodamine B was more subject to **absorption** than Pontacyl Brilliant Pink B when suspended

solids were present, the latter exhibited a high rate of photo-chemical decay and natural background level. For the purposes of this study, using Hamilton tap water, which contains a very low amount of suspended solids, Rhodamine B was chosen as an acceptable tracer.

A stock solution of 1.0 percent Rhodamine B was diluted by adding 36 millilitres and 42 millilitres to 5 litres of tap water to yield feed solutions of 72 and 84 milligrams per litre respectively. Throughout the experiment the feed solution was maintained at the same temperature as the fluid stream entering the test vessel in order to minimize any undesirable convection currents or density gradient effects. The point of tracer injection was in the centre of the influent fluid stream at the inlet weir.

A G.K. Turner and Associates model 111 fluorometer fitted with a continuous sampling cuvette was used to measure tracer concentrations in the effluent stream. Primary filters 1-60 and 58 were used with the secondary filter 23A. The fluorometer was calibrated before and after each experimental test using measured amounts of Rhodamine B in Hamilton tap water. In addition during each test, with the tracer feed pump set at a constant pumpage rate the actual measured concentration of tracer in the test vessel was compared to the theoretical dosage being applied. Typical fluorometer calibration curves are shown in Appendix IV.

Continuous sampling was achieved by fitting a syphon tube to the fluorometer cuvette. This arrangement continuously extracted a part of the effluent stream from the middle of the opening in the discharge weir. At a syphoning rate of 227 cubic centimeters per minute there was an associated time lag of three to four seconds for the liquid sample to reach and activate the fluorometer.

A Honeywell Electronic 19 recorder was used to continuously chart fluorometer readings in terms of millivolts versus time.

In addition to the mixing created in the test vessel by entrance and exit turbulence, mixing was provided during certain test runs by placing a high speed electric mixer in the middle of the tank. The intent of providing this mixing was not to simulate perfect mixing conditions but rather to determine what effect, if any, a greater or lesser degree of turbulence had on test results.

The equipment that has been described was that actually used during this study. Prior to developing this equipment, several other methods of producing and monitoring a sine function were unsuccessfully tested.

Initially a commercially available function generator such as is commonly used in Electrical Engineering work was investigated. Unfortunately, the sine waves produced by the generator were of too high a frequency to produce any useful

output from the system under study. At high frequencies, the response from the experimental vessel was in the form of an irregular line with no defineable peaks and depressions such as are characteristic of the response to a cyclic forcing function. The inadequacy of this method of signal generation is thought to be partially attributable to the fact that the pumping mechanism used was too insensitive to accurately reproduce the signals supplied by the generator. That is, the lag period required for the pump to respond and achieve a new pumpage rate effectively damped out any variations and so a near constant flow of tracer was produced.

An electrolytic pump, activated by a sinusoidally varying current, was also tested as a means of introducing a sine wave disturbance into the experimental vessel. It was found that the compressible nature of the air in the tracer reservoir seriously damped fluctuations in tracer flow. Coupled with this, the altering hydraulic head conditions, as the tracer was forced from the reservoir distorted the signal further and so rendered this equipment useless.

For effluent monitoring purposes, both a fluorometer and a specific ion electrode were tested. In terms of response time and sensitivity the specific ion electrode showed promise of being well suited for monitoring frequency response output. A commercially available (Orion) chloride electrode was used in connection with a calomel reference electrode and

an expanded scale pH meter. In tests using sodium chloride as a tracer and Hamilton tap water as a carrier fluid, this instrument proved capable of registering cyclic output disturbances. However in analysing and interpreting the output data, it became evident that the results were erratic and seemed to indicate unsteady state conditions in the test vessel. Further investigations using only carrier fluid without any tracer added showed that the system response varied considerably with time. This variation with time was not due to temperature fluctuation since the temperature of the carrier fluid was monitored and remained constant.

4.2 Experimental Technique

Three different reaction vessel configurations were investigated in this work. At a chosen tank configuration flow rate and degree of applied mixing were held constant while other variables remained constant and the vessel was again subjected to the same range of sine wave frequencies. This procedure was then repeated at approximately one half the original flow rate.

The vessel initially tested was a rectangular metal trough 97.5 centimeters long and 19.4 centimeters wide. Depth of fluid in the vessel varied according to flow rate. During subsequent tests, the length of the vessel was first altered to provide a tank of approximately twice the original length and then one of approximately half the original

length.

At any one set of conditions the vessel was tested using sine wave disturbances of varying frequency. At each chosen frequency, the system was forced through a sufficient number of complete cycles to ensure that the transient portion of the response curve had been surpassed.

CHAPTER 5

DATA ANALYSIS5.1 Amplitude Ratio

In all experimental tests, effluent concentration was continuously monitored and recorded on the strip chart of a Honeywell Electronic 19 recorder. The concentrations measured in this way were in terms of millivolts versus time. The resulting output curves were then used to get an average of sine wave peak value and sine wave minimum value for each particular frequency. The values in terms of millivolts were converted to concentration of tracer by interpolating from the appropriate fluorometer calibration curve. In this way, values of sine wave amplitude were determined and subsequently converted to a dimensionless amplitude ratio through division by the input value of sine wave amplitude.

5.2 Phase Lag

During the testing procedure, the time of input of the mean value of tracer concentration was noted on the effluent recording chart. From the output curves the time for the effluent concentration to reach this mean value was also noted and the corresponding time difference was calculated. This time difference, representing the relative displacement of the output sine wave from the input sine wave, was used to calculate the phase lag for the system at each particular test frequency. To account for the time lag associated with the delay in activation of the fluorometer, the phase angles

were corrected by subtracting four seconds from the time differential between the mean values of tracer input and output.

In analysing the raw data, the initial portion of the sinusoidal response curve was disregarded as being non representative. This was done to ensure that the transient response portion of the system's output curve had been surpassed. For all practical purposes the transient portion of equation (7) can be assumed to be negligible after a time equal to three times the residence time of the system under study. (5) Also the values of amplitude and phase angle which were determined from the experimental curves are average values which were calculated, in each case, from at least five complete sine wave cycles. The results of the data analyses for all experimental tests are presented in Appendix II.

5.3 Input Waveform

Since the input waveform was not monitored or recorded, the values for input amplitude have to be calculated. The three variables effecting the input sine wave amplitude are flow rate of the carrier fluid, feed concentration of Rhodamine B and maximum and minimum rates of tracer input. The flow rate of carrier fluid and the tracer feed concentration are both known quantities and therefore, by determining the maximum and minimum rates of tracer input from the kinetic clamp pump calibration curve, the input sine wave amplitude

can be determined. Calculations of input amplitudes for each experiment are provided in Appendix I.

5.4 Output Waveform

From strictly a theoretical viewpoint the output from the experimental system is expected to be a sine wave, provided the system has stable, linear characteristics and provided no forms of distortion such as generating or monitoring inadequacies are present. Therefore, in order to apply frequency response analysis with confidence and as a means of partially assessing the linearity of the experimental system, it is necessary to study the characteristics of the output waveforms. This is done by comparing the experimental waveform output to a calculated theoretical sinusoidal system output, the theoretical output being calculated from the relationship

$$C = C_o \sin (wt + \&)$$

where C = output sine wave value (mv)
 C_o = output sine wave amplitude (mv)
 $\&$ = phase angle (negative)
 w = frequency (radians/sec)
 t = time

The value for C_o is taken from the experimental data. Then the values of theoretical and experimental output can be compared at several increments of time covering a complete wave cycle and so a decision can be reached as to whether the experimental output was a sinusoid. Examples of such calculations are given in Appendix III. The comparison is

presented in tabular form and an illustration of a typical input-output sine wave relationship is shown.

These comparisons show that, within a certain range of frequencies, the output waveforms from the experimental systems all conform to the theoretically calculated output sine waves. However at high frequencies such as in Experiment I Run G and Experiment IV Runs A, B, and C the actual system output and the theoretical output do not compare favourably. In these cases, the recorded trace of the output is not a smooth curve as is the case at lower frequencies, but rather exhibits random jagged peaks and flat spots so that there is no continuity of waveform characteristics from one cycle to the next. The output waves are definitely cyclic in nature and of equal period but they do not conform to the characteristics of the expected sinusoidal response.

This non-conformity to sinusoidal characteristics is not likely due to system non-linearities since, with inputs of lower frequency, the same systems did respond in a sinusoidal manner. Other possible sources of distortion of the output wave could perhaps be attributed to the signal generating device or the effluent monitoring apparatus. The most likely of these two possibilities would seem to be the fluorometer which was used to monitor the effluent tracer concentration.

As noted previously there was approximately a four

second time delay from the time of sample extraction from the effluent stream until the sample reached the fluorometer cuvette and so produced a fluorometer response.

To reach and activate the fluorometer the fluid travelled through a small diameter syphoning tube which abruptly expanded at the entrance to the larger diameter cuvette. Now if the sampling procedure can be thought of as continuously removing successive discrete small quantities or "packets" of fluid from the effluent stream then it is possible that the turbulent entrance conditions at the mouth of the cuvette could have resulted in a re-arrangement of the time order in which the small "packets" of fluid activated the fluorometer. Also, since the cross sectional area of the cuvette was much greater than that of the syphoning tube it is likely that the fluorometer readings resulted from several "packets" of fluid activating the fluorometer simultaneously.

If this were the case the system output at all frequencies would be subject to the same distortion. However the distortion created would be most evident in the higher frequencies since for equal time increments a high frequency wave will have passed through more degrees and therefore a greater range of tracer concentrations than a low frequency wave. For example in a four second interval, the output concentration of a sine wave with a period of 30 seconds could have changed by as much as 40% of the peak amplitude while in the

same interval a wave with a period of 180 seconds will have traversed only 7% of the amplitude scale. This then would account for the lack of noticeable distortion at low frequencies and the evident increase in distortion as the sine wave frequency increased.

In general, all the recorded output waves with periods of 60 seconds or less were distorted and did not exhibit recognizable sinusoidal characteristics. The amplitudes recorded for these outputs represent average values only and it should be realized that the actual amplitude of any one wave could have exceeded or fallen short of this value by as much as 50%. Therefore, it is felt that these data points do not represent a true picture of system response and cannot be used with any confidence. For this reason these data points are not considered in analysing or describing the experimental systems.

The only other waveform which did not display sinusoidal characteristics was that arising from Experiment III Test Run A. In this case the sine wave generating device was at fault since at very low frequencies the gear reducer tended to slip and so the angular momentum supplied to the drive mechanism was not constant. Therefore, while the average sine wave period during the test was 860 seconds, this value varied from 765 seconds to 885 seconds and so the resultant data, being non-constant, cannot be used for further analysis.

CHAPTER 6

EXPERIMENTAL RESULTS6.1 General

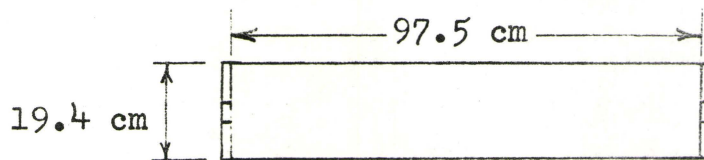
Three arbitrary vessel configurations, A, B, and C, as shown in Figure 4 were tested. In Experiment I, Vessel A was tested with a fluid residence time of 59.3 seconds. The characteristics of the vessel were studied both with and without artificial mixing being provided. Similarly in Experiment II, Vessel A was used with a fluid residence time of 113.5 seconds and again separate tests were made with the flash mixer off and then on. In Experiment III, Vessel B was used with a fluid retention time of 109 seconds and no mixing was provided. Experiment IV was carried out in Vessel C with a fluid residence time of 30.8 seconds with no mixing provided.

The data gathered from Experiments I, II, and III is presented in the form of Bode plots. The data from Experiment IV is not included in this presentation since the validity of three of the high frequency data points is questionable.

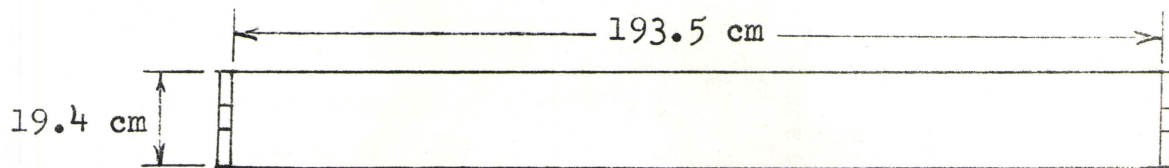
When examining these plots, it should be realized that the experimental data, as presented, has not been subjected to any rigorous analyses to obtain a line of best fit. Rather, the amplitude and phase angle curves which are shown are intended only to more clearly illustrate the general trend or curve shape suggested by the experimental data points.

This unsophisticated approach to data handling and

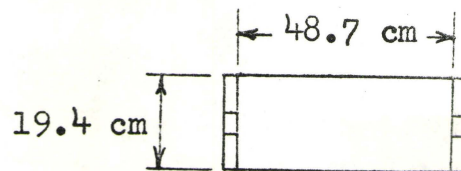
FIGURE 4
TEST VESSEL CONFIGURATIONS



VESSEL A



VESSEL B



VESSEL C

presentation is compatible with the exploratory purpose of this work, and reflects the opinion that the precision of the experimental measurements does not warrant application of a more exact method of data analysis. Also, in keeping with the feasibility approach to this study and for the reasons as outlined above, no attempt is made to develop complex definitive models. Rather, the models which are postulated only approximate the experimental findings but do clearly illustrate the flexibility and ease of modeling that is afforded by the use of a Bode plot representation of frequency response information.

6.2 Experiments I and II - No Mixing Provided

The Bode plots in Figures 5A and 5B show a comparison of the response from the test system of Experiment I to the system used in Experiment II. The high speed mixer was not used in either case. The actual reactors tested are physically identical with the only difference being in flow rate of carrier fluid or in other words, fluid residence time. In Experiment I, the test vessel has a residence time of 59.3 seconds while in Experiment II, the residence time is 113.5 seconds.

From Figure 5A, which shows the relation of amplitude ratio to frequency, it can be seen that the curves for both Experiment I and II show a general resemblance to the Bode plot for a completely mixed tank. However Figure 5B, showing phase lag as a function of frequency, has none of the charac-

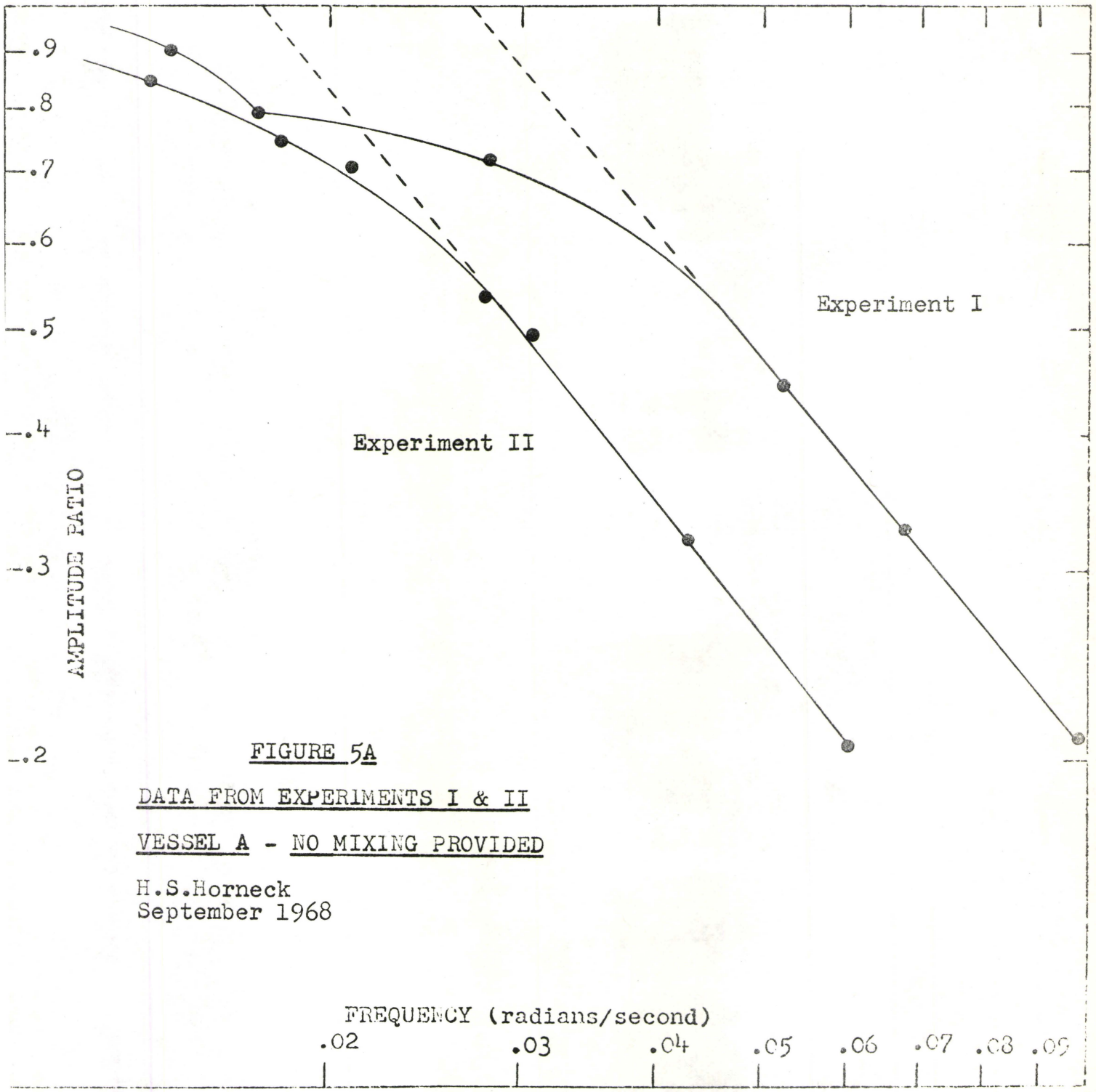
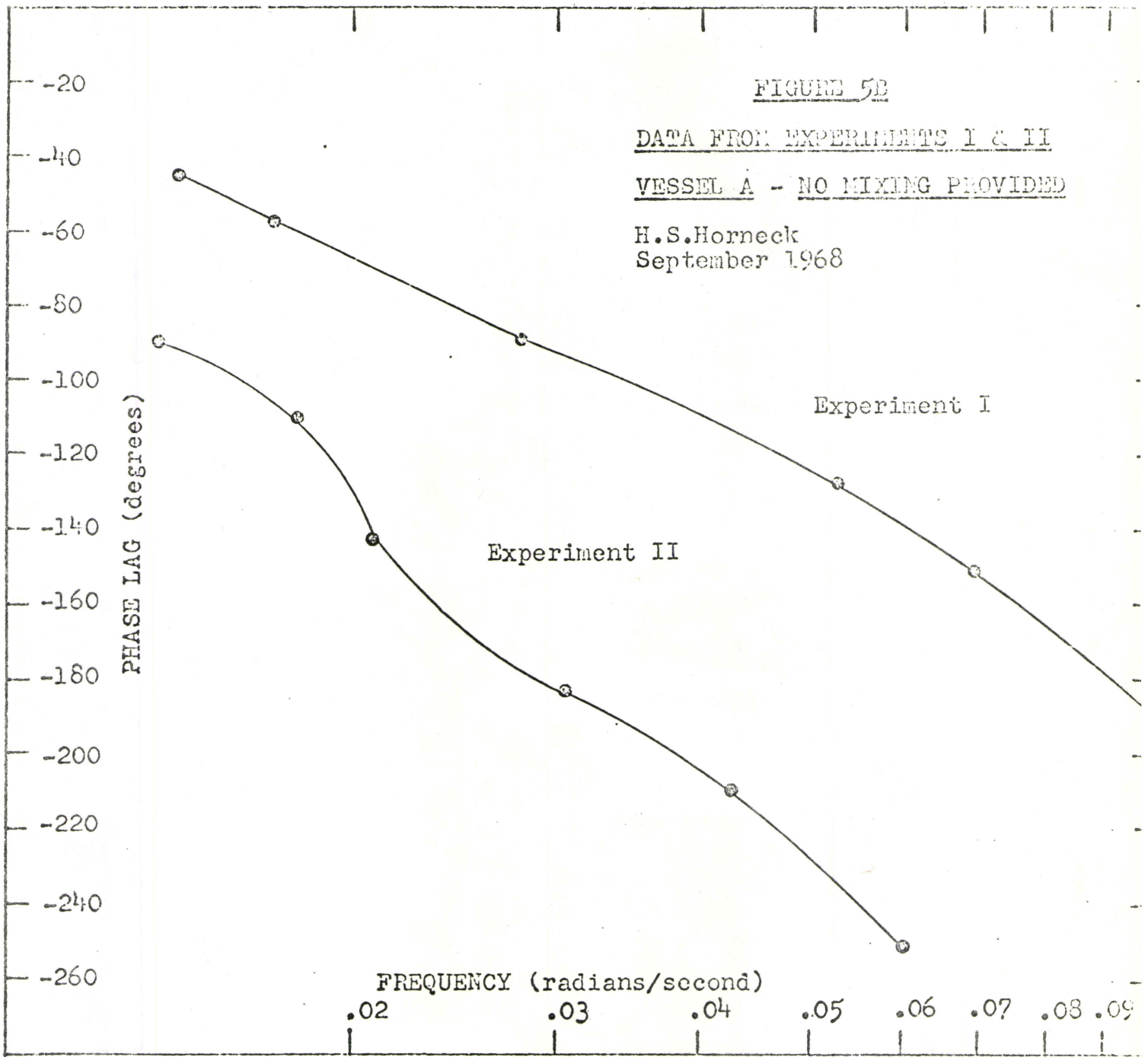


FIGURE 5A

DATA FROM EXPERIMENTS I & II

VESSEL A - NO MIXING PROVIDED

H.S.Horneck
September 1968



teristics common to the phase lag curve representing a completely mixed tank. This curve does not have the characteristic symmetry about asymptotes at 0° and -90° but instead the phase lag increases steadily with increasing frequencies.

From these Bode plots it is evident that the partially mixed systems investigated in Experiments I and II cannot be adequately described only in terms of a completely mixed vessel. The other extreme would be to compare the experimental results to the theoretical output from a plug flow reactor.

To do this it has been shown that a plug flow reactor can be successfully modeled by a cascade of n perfect mixers of total volume V such that each reactor has a volume V/n . If the constant flowrate q is the same to each reactor, then the transfer function for the cascade is:

$$G(s) = \left[\frac{1}{(\tau_0/n)s + 1} \right]^n$$

where $\tau_0 = \frac{V}{q}$

From this the magnitude and phase angle are

$$|G(j\omega)| = \frac{1}{(1 + (\omega\tau_0/n)^2)^{1/2}}$$

$$\angle G(j\omega) = -n \arctan(\omega\tau_0/n)$$

Now as n approaches infinity

$$|G(j\omega)| \rightarrow 1$$

and $\angle G(j\omega) \rightarrow -\omega\tau_0$

This would then yield a Bode plot with an amplitude ratio of 1 at any frequency and this obviously does not

relate well to the results shown in Figure 5A. However the phase lag for a plug flow reactor will increase steadily with increasing frequencies so that the phase lag plots of Figure 5B more closely resemble the response from a plug flow reactor than from a perfectly mixed reactor.

Since the amplitude plot resembles that of a CSTR, and the phase lag plot has characteristics which resemble a PFTR response, it is reasonable both from a theoretical and a practical viewpoint to think of the test reactor as operating somewhere between these two extremes. A mixed model in which a certain part of the experimental reactor was perfectly mixed with the remaining volume being plug flow could therefore possibly describe the system output.

To model on this basis requires an initial estimate of the percentage of reactor volume which is completely mixed or which acts as a plug flow reactor. A rough estimate of volume split can be arrived at in one of two ways. First the asymptote of the straight line portion of the amplitude plot could be extended to meet the line representing unit amplitude ratio. The frequency at this point is equal to the reciprocal of the residence time of fluid in the mixed portion of the vessel. Alternatively, at high frequencies the experimental phase lag can be used to estimate the residence time of fluid in the plug flow portion of the tank. This is possible since at high frequencies the phase lag for a mixed

vessel approaches 90° , so that any angle in excess of this can be attributed to plug flow and equated to $w\tau_{PFTR}$ where τ_{PFTR} is the residence time of the plug flow portion of the reactor.

6.2.1 Models 1 and 2

This modeling procedure can be illustrated by attempting to theoretically produce the plots in Figures 5A and 5B which represent the test vessel used in Experiment 1 when no mixing was provided.

From the amplitude plot

$$1/\tau_{CSTR} = .0275$$

$$\tau_{CSTR} = 36.5 \text{ seconds}$$

$$\begin{aligned} \text{therefore } \tau_{PFTR} &= \tau_{\text{total}} - \tau_{CSTR} \\ &= 59.3 - 36.5 \\ &= 22.8 \text{ seconds} \end{aligned}$$

Alternatively from the phase lag plot at $w = .09$

$$\angle G(jw)_{CSTR} + \angle G(jw)_{PFTR} = -174^\circ$$

$$\begin{aligned} \text{or } \angle G(jw)_{PFTR} &= -174^\circ + 90^\circ \\ &= -84^\circ \end{aligned}$$

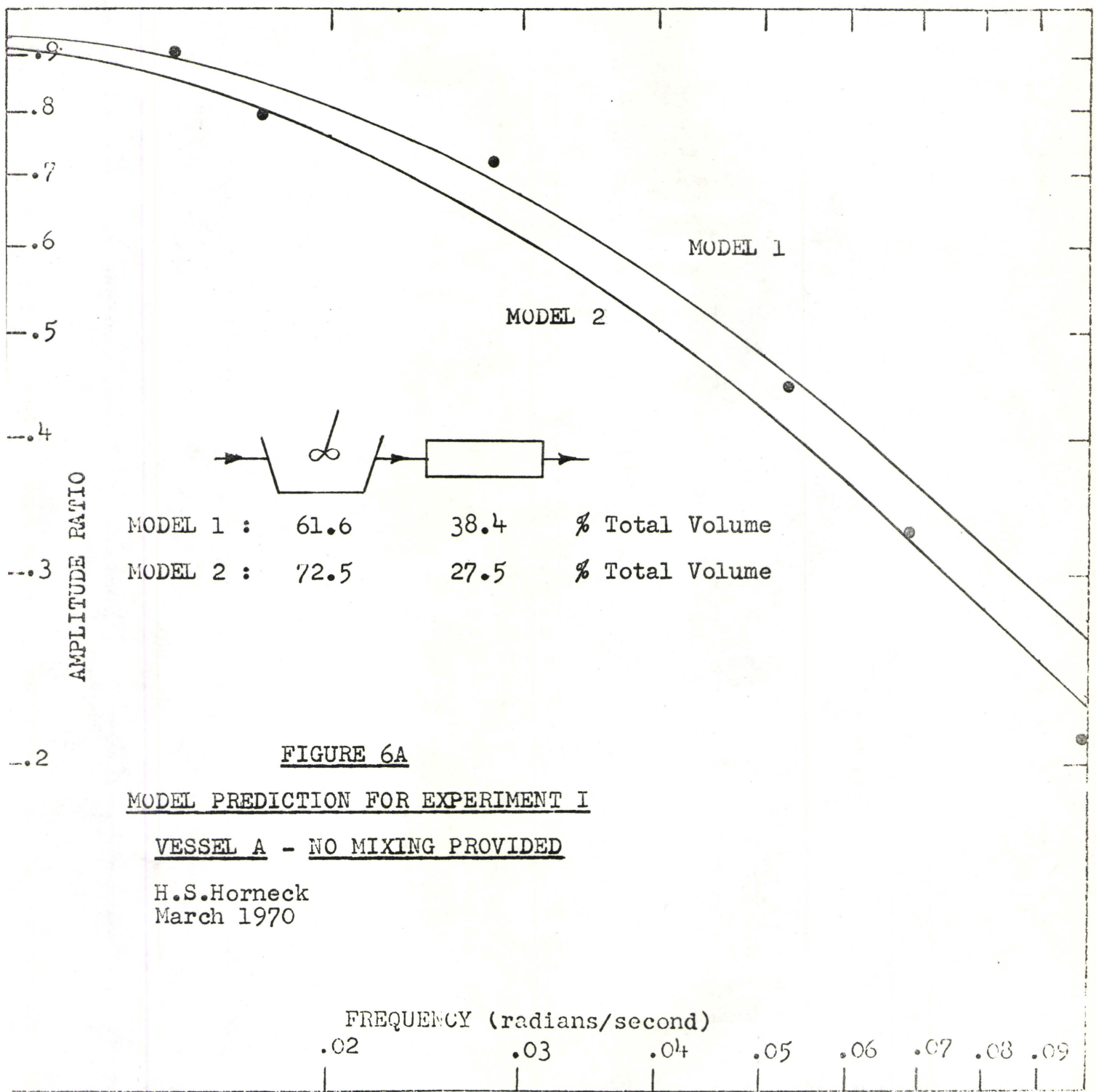
$$\text{therefore } -\tau_{PFTR} w = -84^\circ$$

$$\text{or } \tau_{PFTR} = 16.3 \text{ seconds}$$

$$\begin{aligned} \text{then } \tau_{CSTR} &= 59.3 - 16.3 \\ &= 43 \text{ seconds} \end{aligned}$$

Now if Bode plots for these two estimated volume splits are constructed (calculations in Appendix V) the results are as shown on Figures 6A and 6B.

From these figures it can be seen that neither theoretical



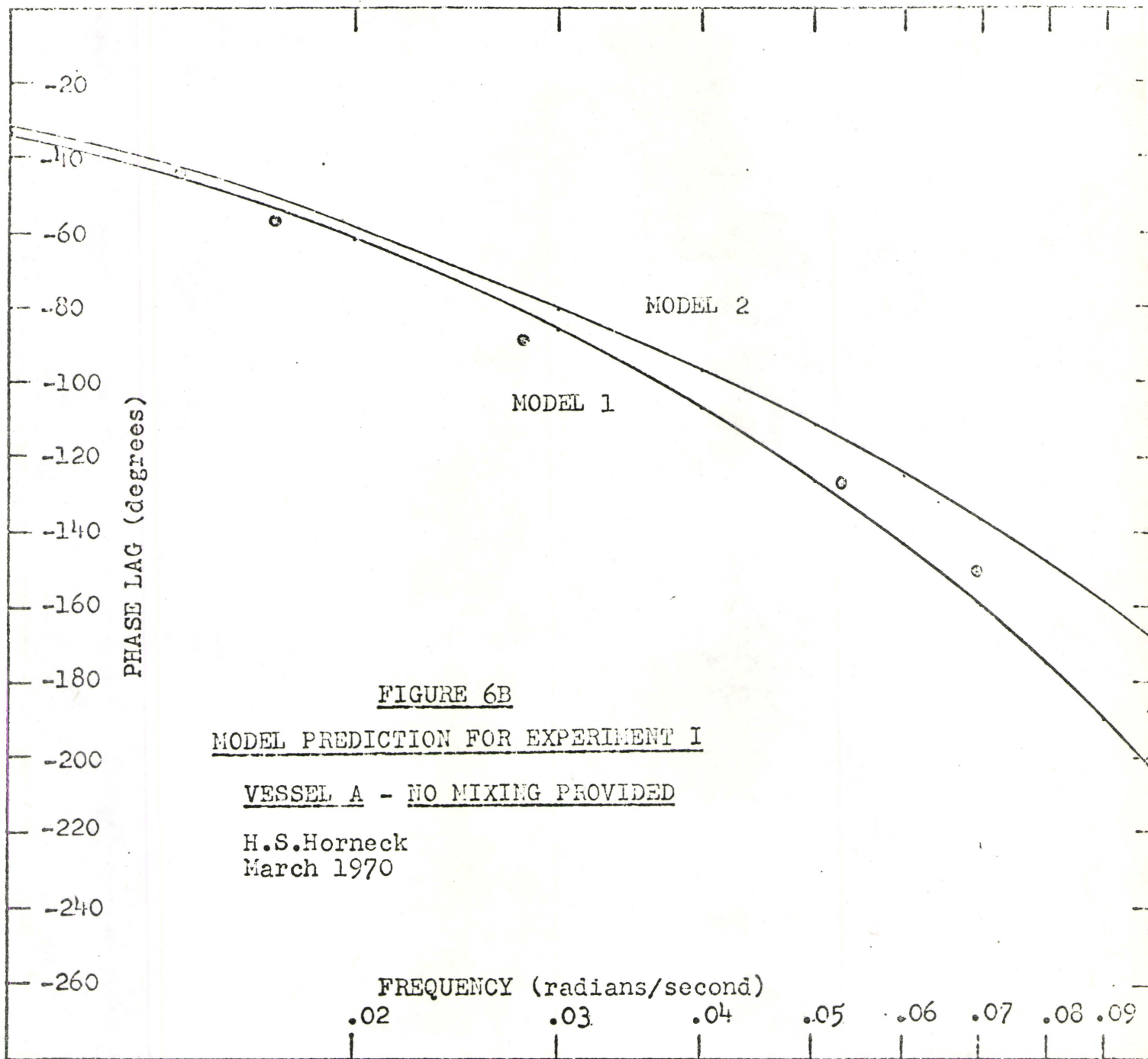


FIGURE 6B

MODEL PREDICTION FOR EXPERIMENT I

VESSEL A - NO MIXING PROVIDED

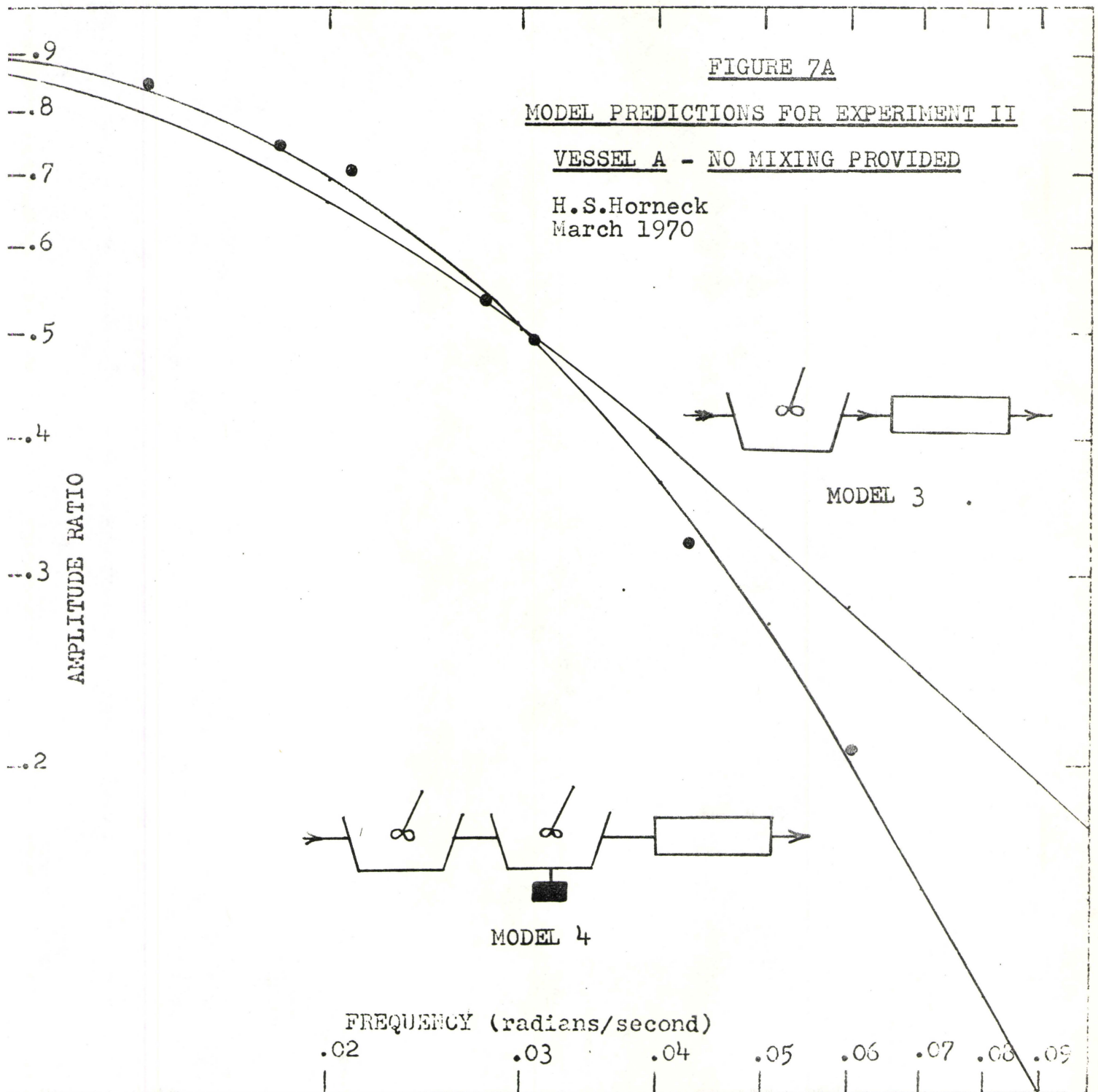
H.S.Horneck
March 1970

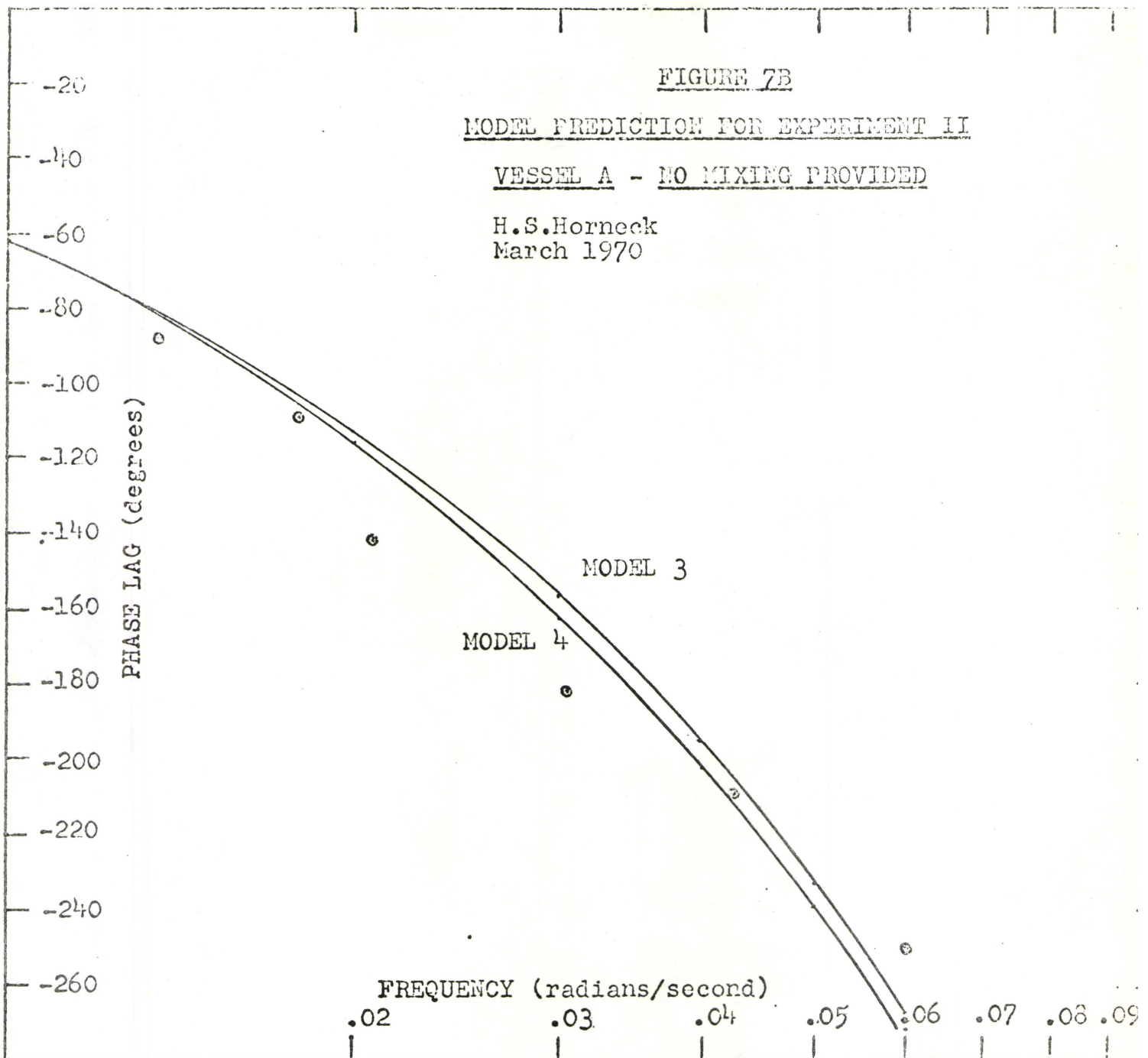
model fits the experimental findings correctly. In particular there is quite a wide divergence in the amplitude plot which arises from the fact that the experimental plot had a negative slope greater than one while both theoretical plots had a slope of -1 since they represented ideally mixed vessels. However, the composite theoretical phase angle plots do compare quite closely to the experimental plot and the two postulated models provide a type of envelope within which most of the experimental data points are contained.

Although the postulated models in this case do not closely compare with the test system this is not unexpected. A more complex model and an iterative technique to closely define volume splits would likely produce closer results. Still this example is useful to point out the ease with which different models can be developed and tested.

6.2.2 Models 3 and 4

Treating the data from Experiment II in the same manner Model 3 can be developed as shown in Figures 7A and 7B. This model, derived from an asymptotic approximation of flow splits, is composed of a CSTR with a 57 second detention time in series with a PFTR having a detention time of 56.5 seconds. The fit provided by this model is especially poor in the high frequency portion of the amplitude plot. This again arises from the fact that the experimental amplitude plot has a negative slope larger than -1 , so that a single





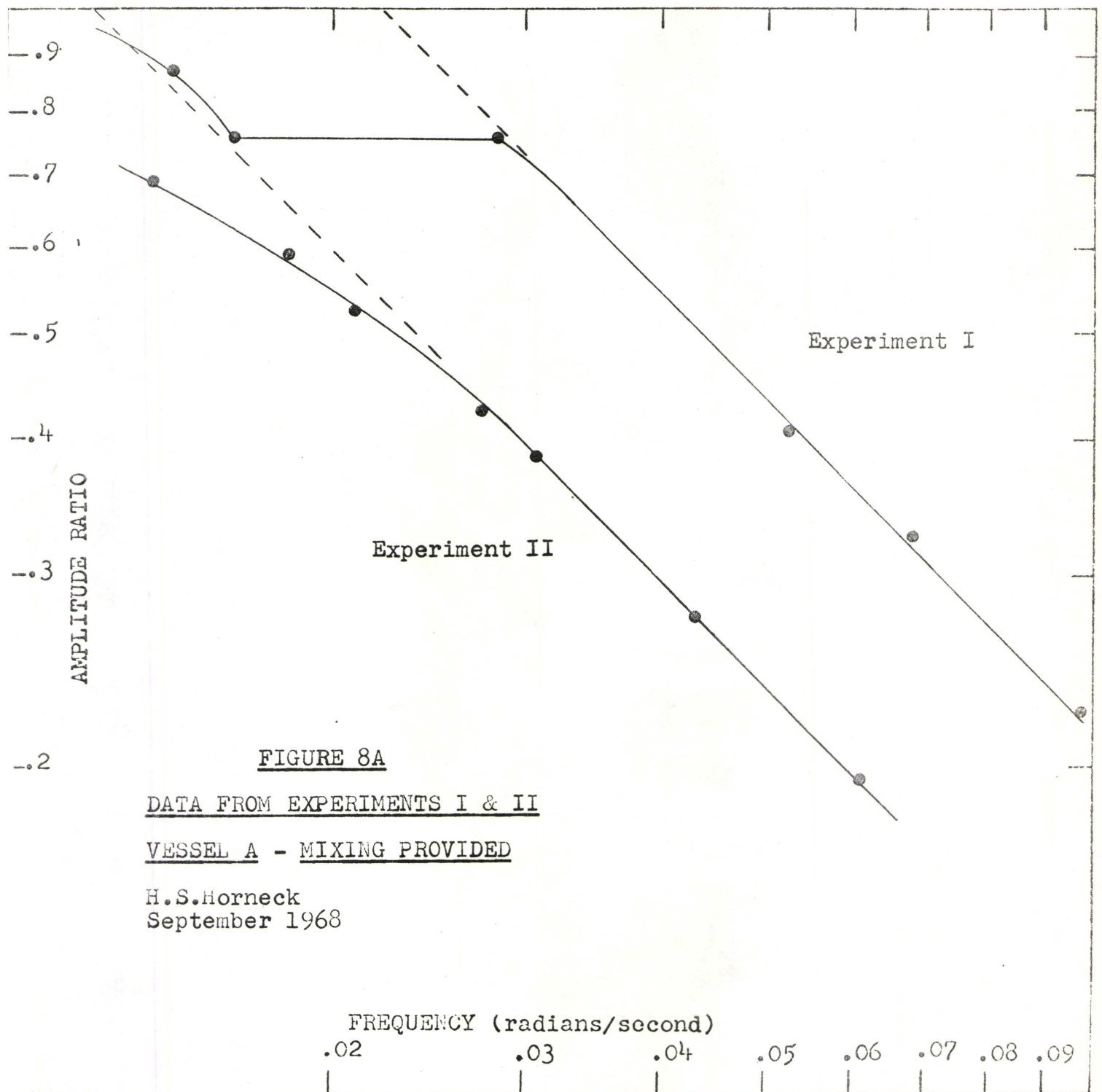
CSTR will not provide good correlation.

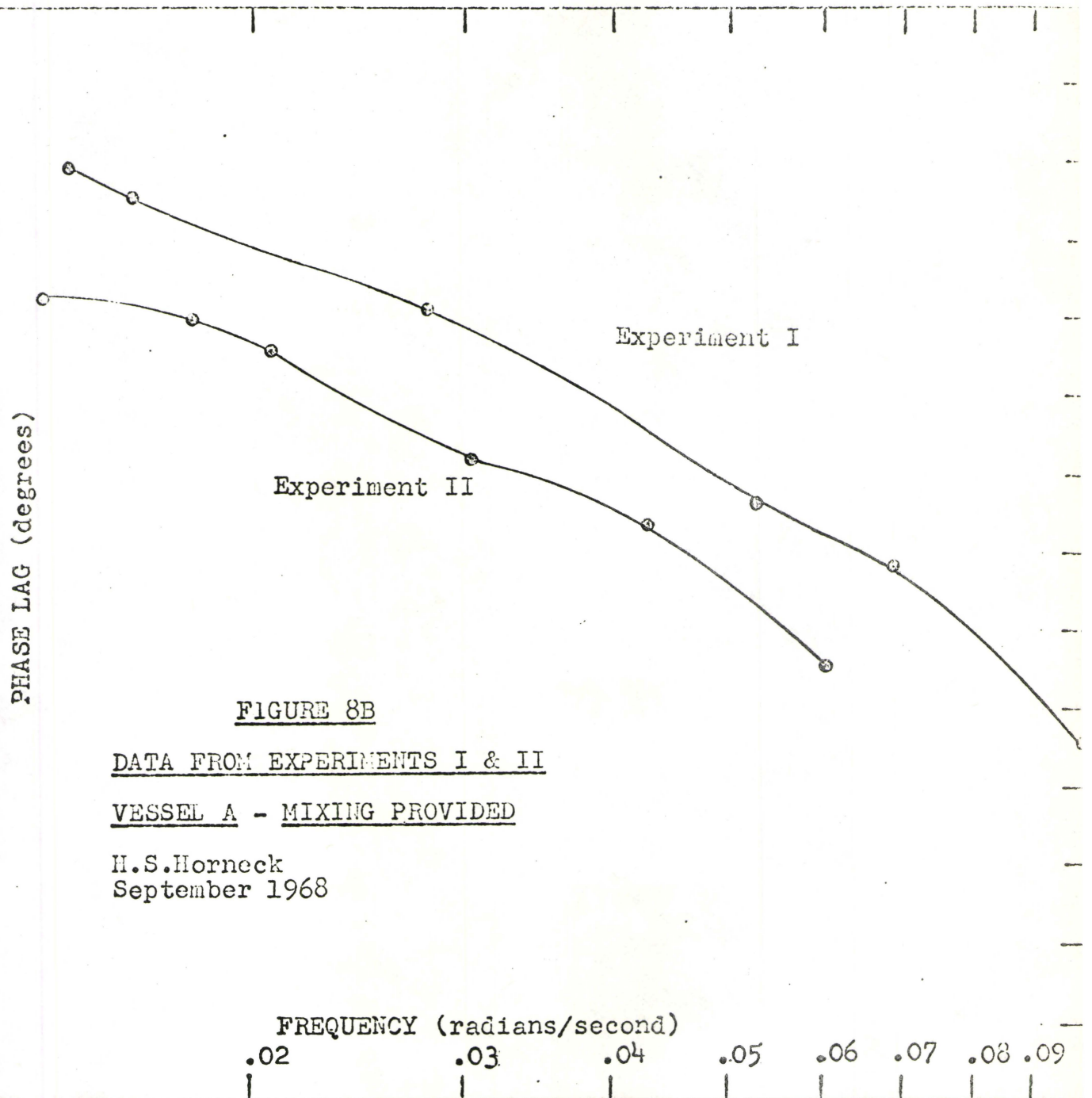
If the experimental data is approximated by two straight line segments representing two CSTR's in series, the amplitude plot can be provided with a better fit. The retention time then in the first CSTR is 37 seconds and in the second CSTR, 30 seconds. Also, to approximate the experimental phase lag the retention time in the in series PFTR is reduced to 42 seconds. This provides a model vessel with a total retention time of 109 seconds. The remaining 4.5 seconds is allotted to dead space. The only effect dead space has in the vessel is one of reducing the total fluid retention time.

Model 4, in Figures 7A and 7B has been developed on the above basis. This model closely approximates the experimental amplitude plot and is equally as good as Model 3 in defining the phase lag plot. This model illustrates the ease and flexibility in modeling with a multi-component system. The amplitude plots for both of the CSTR components in the model were separately plotted and then graphically combined to produce the composite plot in Figure 7A.

6.3 Experiments I and II -- Mixing Provided

The Bode plots shown in Figures 8A and 8B compare the results of Experiments I and II. All test conditions were identical to those outlined for Figures 5A and 5B except that in this case the high speed mixer was used. As would be expected, the amplitude plots show that the system more





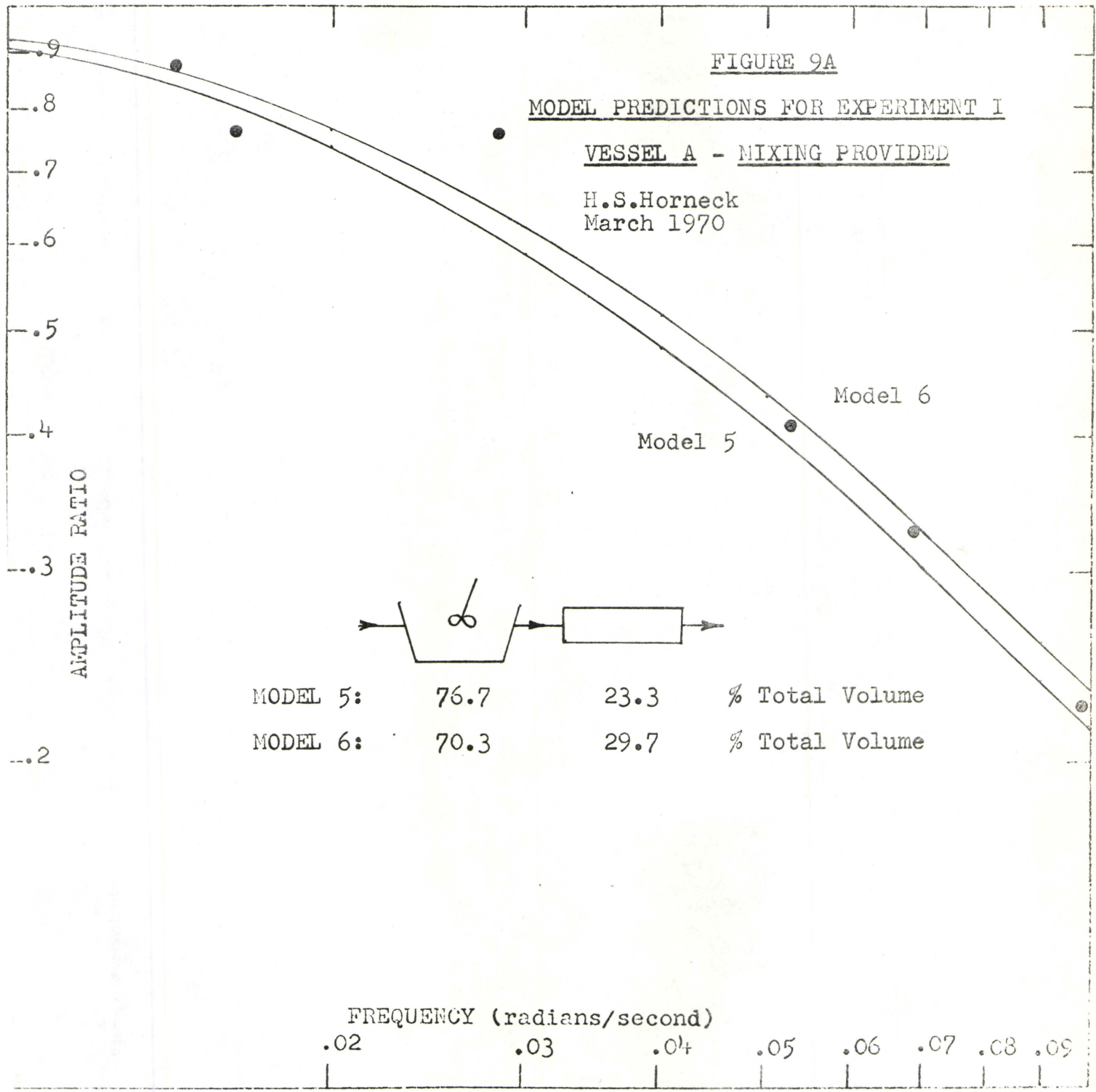
closely approached ideal mixing conditions. This is evidenced by the fact that the slope of the straight line portion of the amplitude plot is approximately -1 as is the case for the response from a CSTR. However, again, the phase lag plots show an increasing phase lag with increasing frequency as is characteristic of the response from a PFTR.

6.3.1 Models 5 and 6

The experimental data from Experiment I indicates a corner frequency of approximately .022 radians per second. Model 5 was therefore developed as a CSTR with a residence time of 45.5 seconds in series with a PFTR having a residence time of 13.8 seconds. The theoretical response from this model, is shown in Figures 9A and 9B. The area of widest divergence between the theoretical and experimental points is in the high frequency portion of the phase lag plot. A closer approximation is provided by increasing the residence time of the PFTR segment to 17.6 seconds and decreasing the residence time in the CSTR segment to 41.7 seconds. This configuration, Model 6, seems to offer a better fit both in the amplitude ratio and phase lag portions of the experimental Bode plot. The development of both these models is documented in Appendix V.

6.3.2 Models 7 and 8

For Experiment II, with mixing provided, the experimental data is approximated by Model 7, which is a mixed model



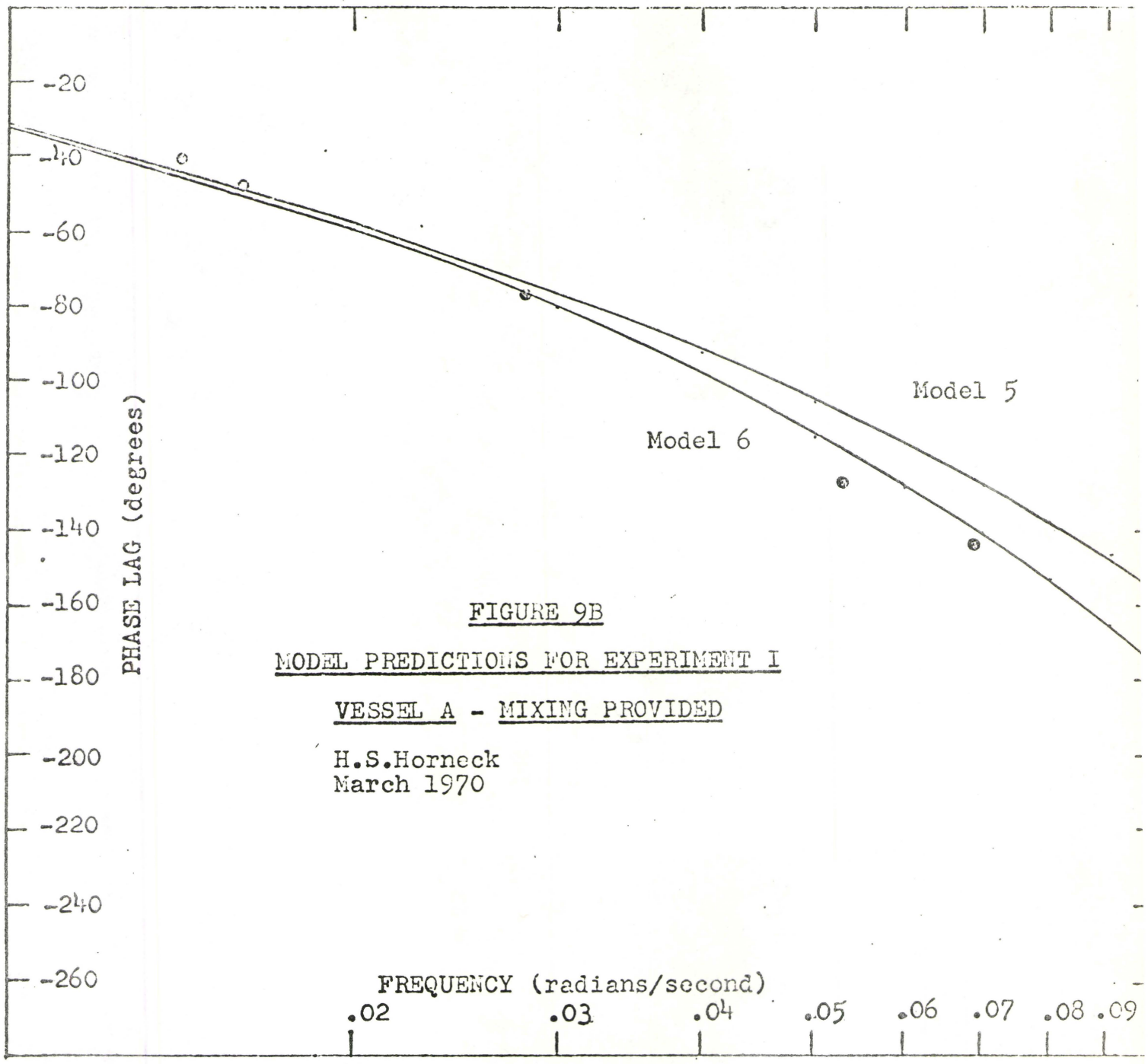
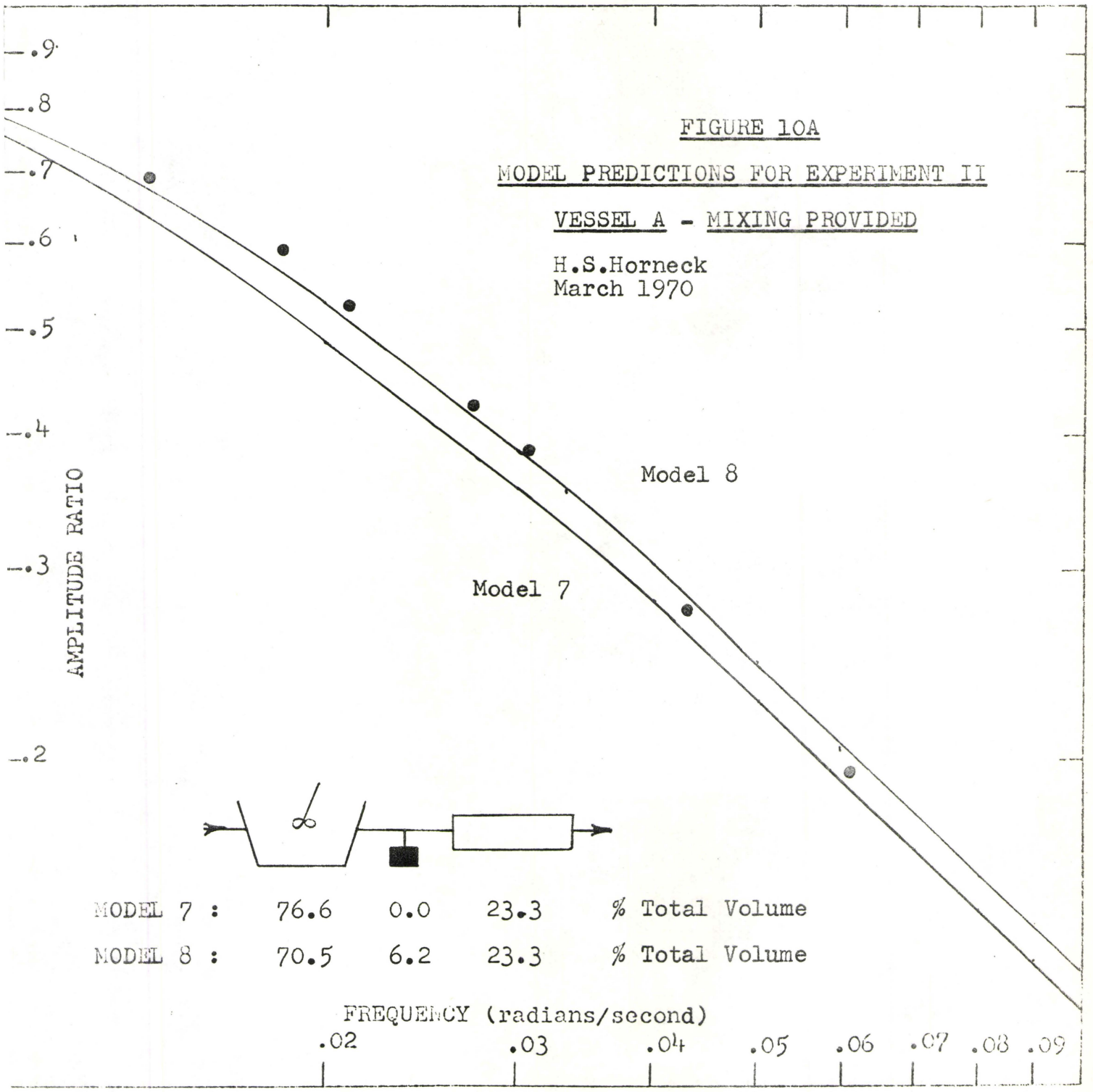


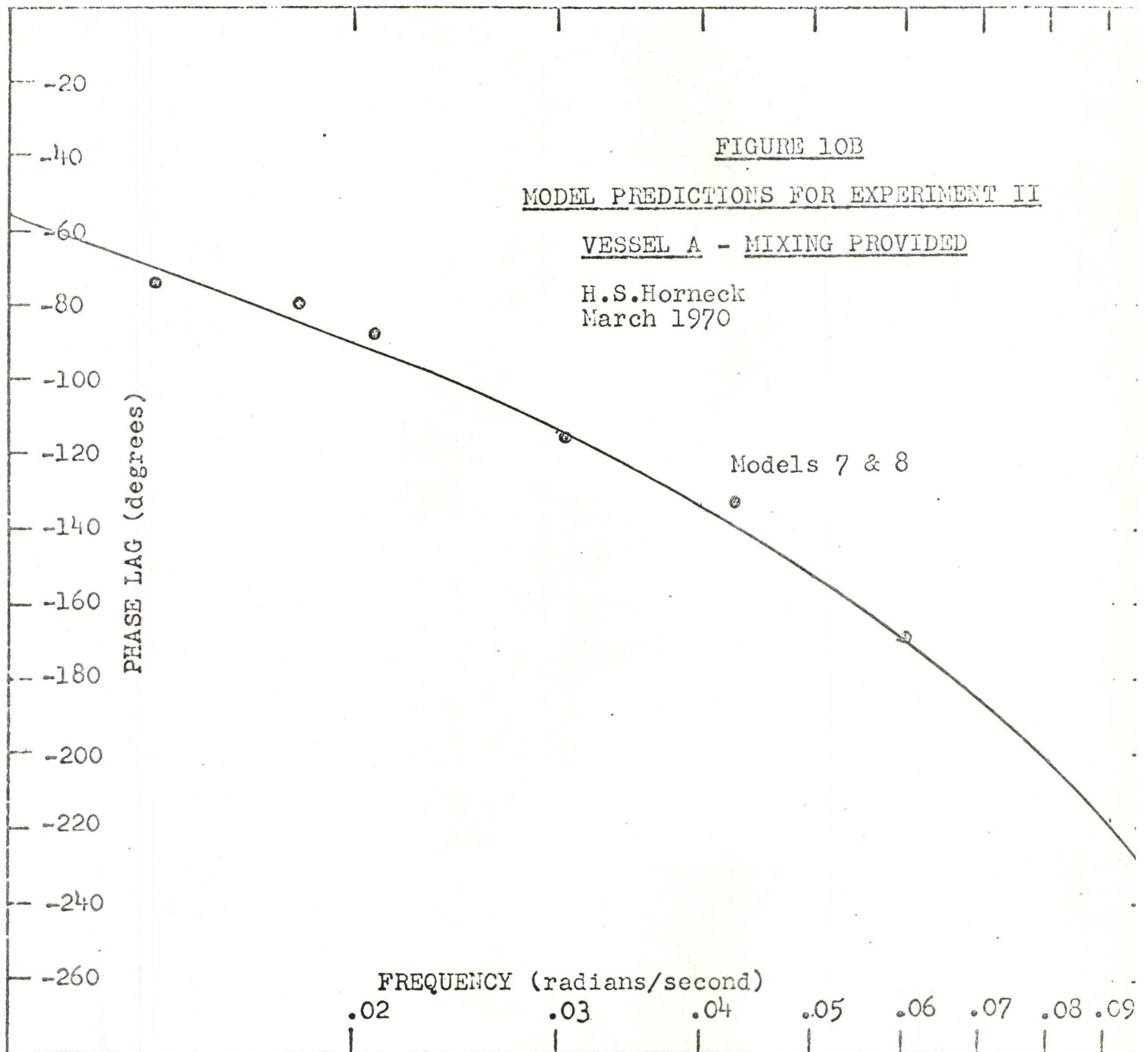
FIGURE 9B

MODEL PREDICTIONS FOR EXPERIMENT I

VESSEL A - MIXING PROVIDED

H.S.Horneck
March 1970





consisting of a plug flow component with a fluid detention time of 26.5 seconds in series with a CSTR segment with an 87 second retention time. This corresponds to a vessel with approximately 77 percent of the fluid volume completely mixed and 23 percent of the volume acting as a PFTR.

The response predicted by Model 7 is shown in Figures 10A and 10B. The phase lag prediction closely follows the experimental data points. The amplitude ratio predictions also resemble the curve shape suggested by the data points but the predicted ratios appear to be consistently low. This would suggest that the CSTR portion of the model is too large.

If the total residence time of the system is reduced by introducing a dead space allowance into the model, then the volume of the CSTR segment can be reduced without affecting the PFTR volume. This is done in Model 8, which provided a better amplitude ratio fit than Model 7. At the same time the phase lag plot has not been adversely affected but remains essentially the same as that predicted by Model 7.

6.4 Experiment III -- No Mixing Provided

Experiment III investigated the response from vessel configuration B with a total residence time of 109 seconds. No artificial mixing was induced. The results of this investigation are shown as Bode plots in Figures 11A and 11B.

The slope of the high frequency portion of the amplitude plot in this case approaches -2. This would indicate a system

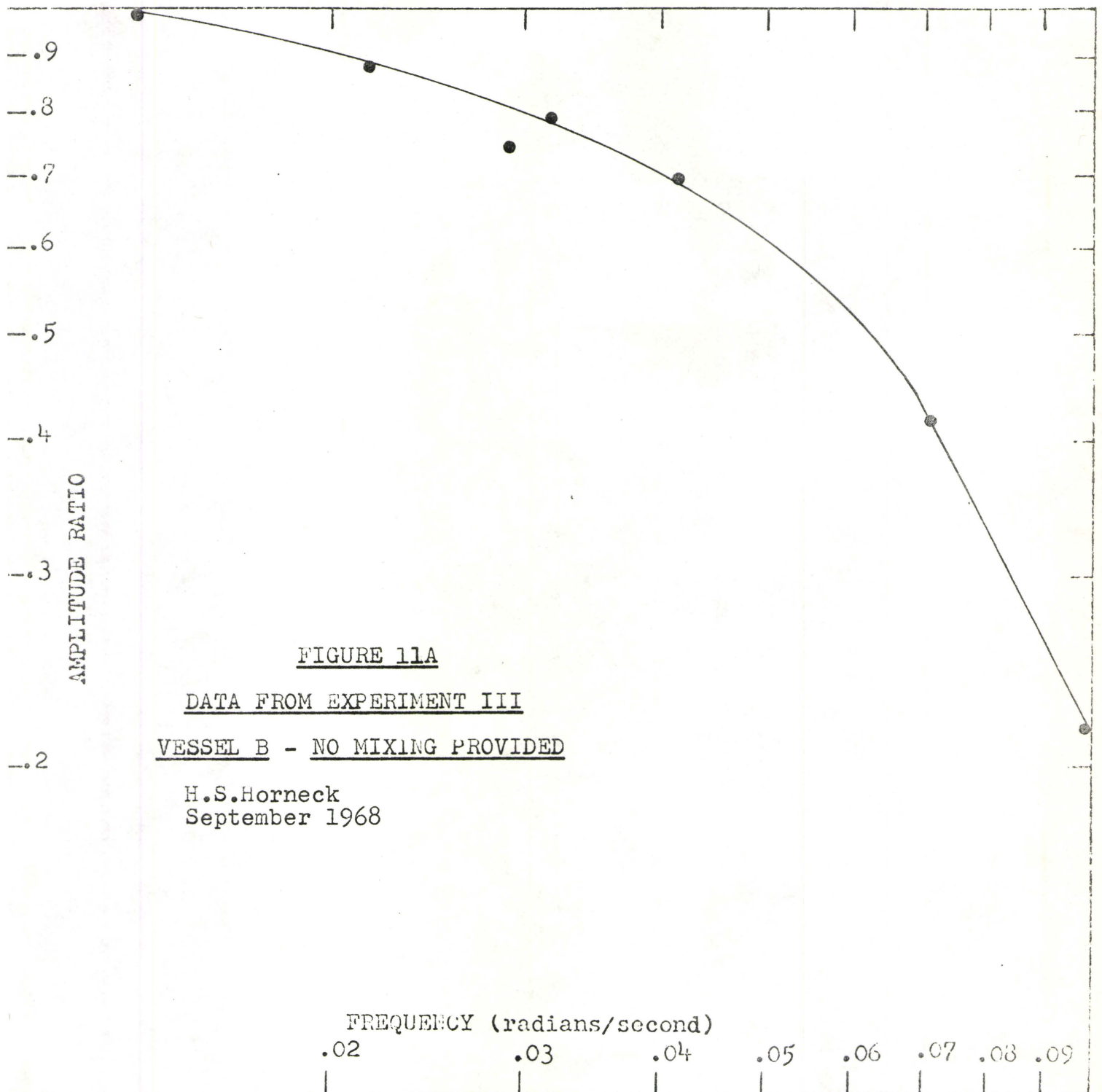


FIGURE 11A

DATA FROM EXPERIMENT III

VESSEL B - NO MIXING PROVIDED

H.S.Horneck
September 1968

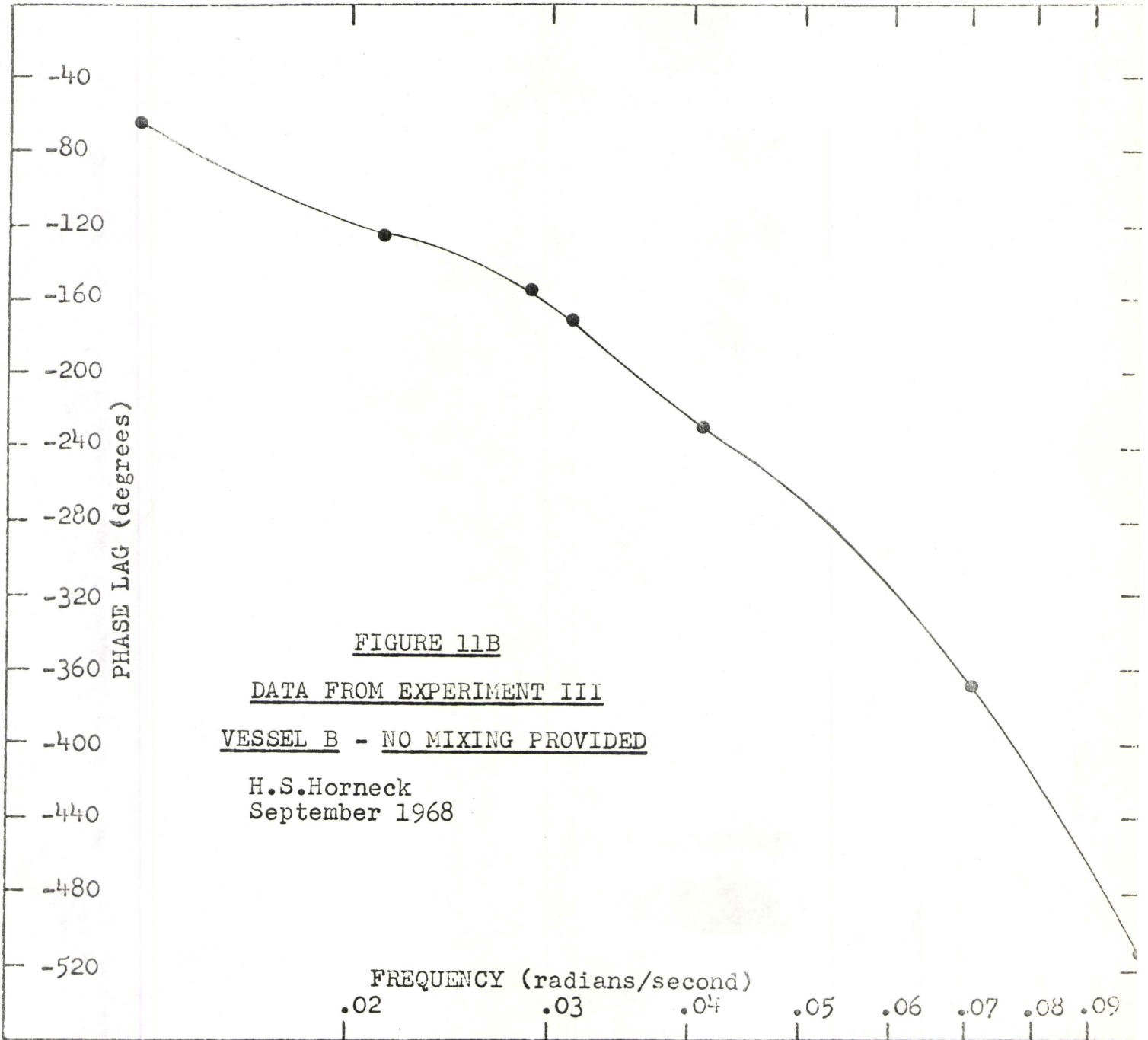


FIGURE 11B

DATA FROM EXPERIMENT III

VESSEL B - NO MIXING PROVIDED

H.S.Horneck
September 1968

composed of two CSTR segments in series. The phase lag presentation shows that as the frequency increases, the phase lag rapidly increases. This would indicate that a fairly large portion of the test vessel was functioning as a PFTR.

6.4.1 Model 8

Figure 12A illustrates the amplitude ratio prediction of two CSTR's in series having residence times of 22 seconds and 15 seconds. The fluid residence time in these two segments was estimated by taking the inverse of the corner frequencies suggested by asymptotic approximation of the experimental amplitude plot. In series with the two CSTR segments is a PFTR having a residence time of 65 seconds. The 7 second discrepancy in residence times between the experimental system and the model is accounted for by introducing a dead space segment into the model. As evidenced in Figure 12B, this model provides quite good correlation with the experimental phase lag data.

6.5 Discussion

6.5.1 Amplitude Ratio

As mentioned previously the amplitude plots were constructed by comparing the average amplitude from at least five complete output sine waves to the theoretically calculated input amplitude. The resultant experimental amplitude reduction can be attributed to the completely mixed regions of the test vessel since, theoretically, any plug flow seg-

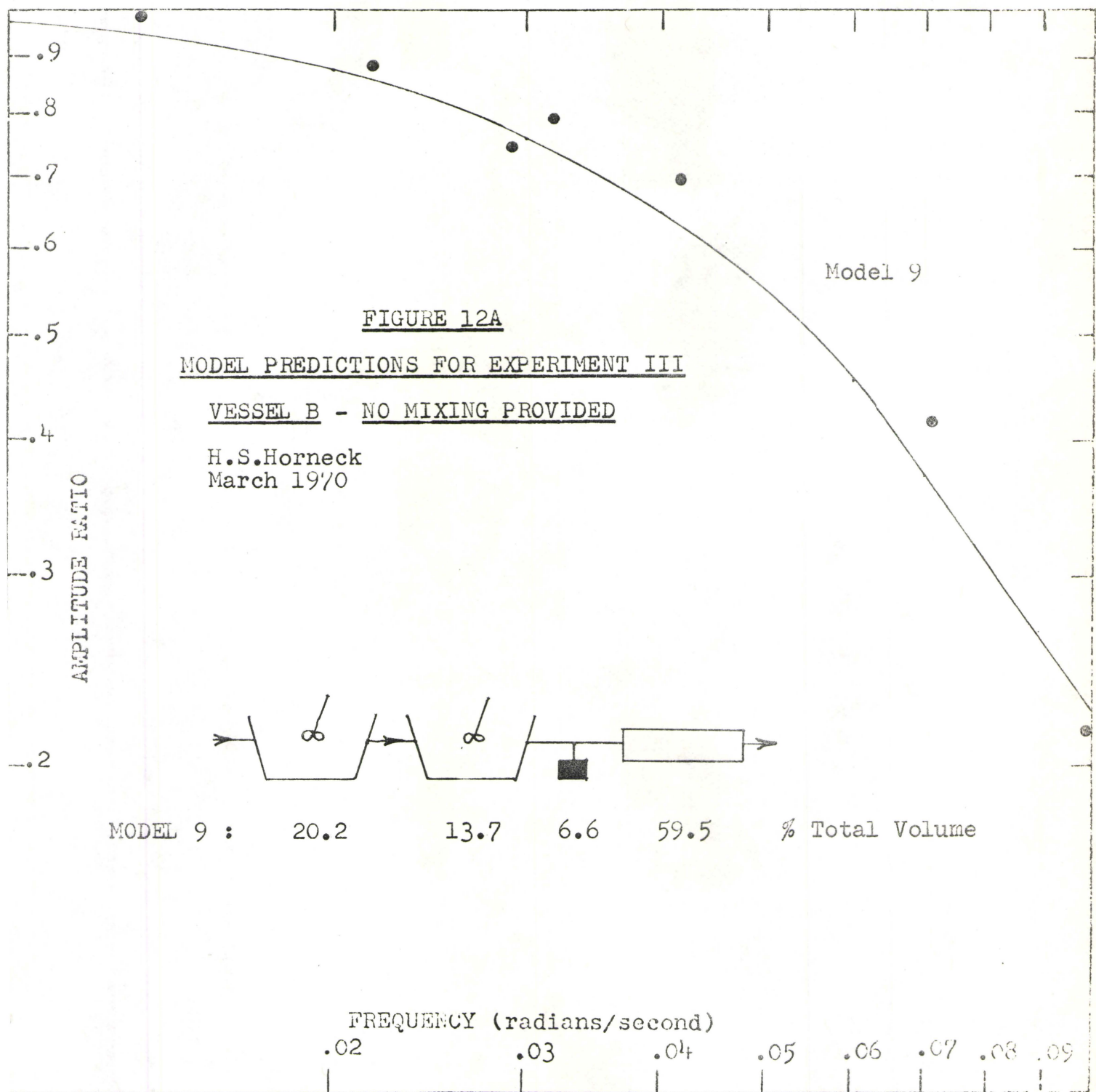


FIGURE 12A

MODEL PREDICTIONS FOR EXPERIMENT III

VESSEL B - NO MIXING PROVIDED

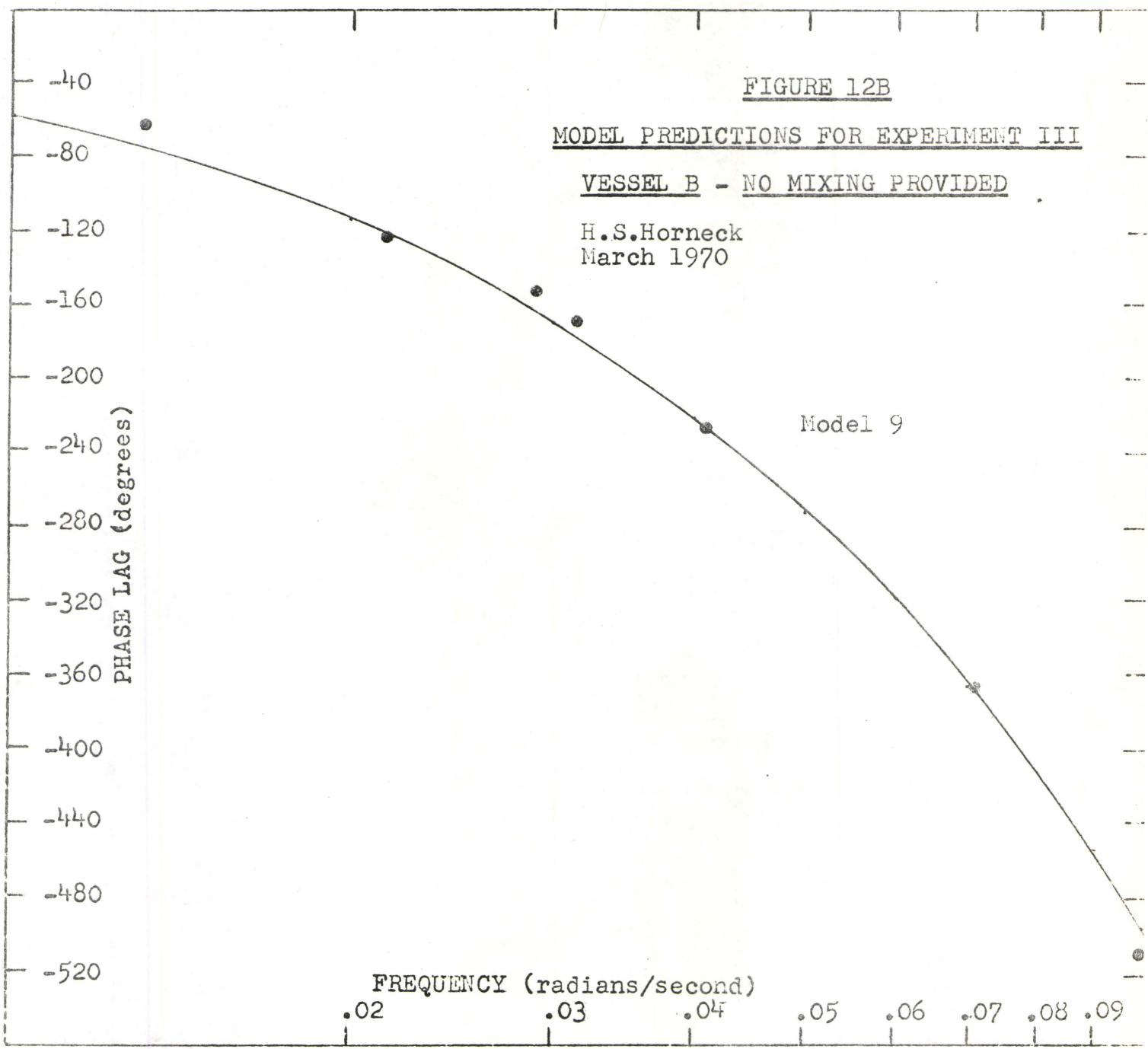
H.S.Horneck
March 1970

Model 9

MODEL 9 : 20.2 13.7 6.6 59.5 % Total Volume

FREQUENCY (radians/second)

.02 .03 .04 .05 .06 .07 .08 .09



ments of the test vessel will not affect the system's amplitude ratio. However, it should be noted that the fluorometer monitoring apparatus can be thought of as a small test vessel in itself with a fluid retention time of 3 to 4 seconds. If mixing occurred in the sampling tube, cuvette arrangement, then the recorded output amplitudes are the combined result of the properties of the test vessel and the monitoring system.

The output wave distortion experienced at high test frequencies, as discussed previously, is thought to be mainly attributed to the effluent monitoring system. This is a limiting factor in analysing and describing the test vessels since, due to a restricted range of test frequencies, the final slope of the high frequency portion of the amplitude plot cannot be defined with confidence. This portion of the amplitude ratio curve is of prime importance when using asymptotic approximations to determine the number of CSTB's in the model configuration.

3.5.2 Phase Lag

Phase lag determinations are normally thought of as the degrees of displacement between the peak of the input sine wave and the peak of the system response sine wave. If experimental phase lags are determined in this manner, a substantial error can be introduced in attempting to locate the exact peak of both the input and output waveforms.

In this work the phase lag determinations were made by graphically measuring the displacement of the average value of the output sine wave from that of the input sine wave. The horizontal axis through the output sine waves can be easily determined from the average values of several peaks and low points of the experiment output. Using this method, there is no need to locate the exact peak of the waveforms and it is felt that the experimental error in determining experimental phase lags is reduced. The accuracy of both phase lag and amplitude ratio determinations could be enhanced by monitoring both the input and output sine waves and simultaneously recording these on a two channel recorder.

6.5.3 Modeling

A successful model configuration should produce a response that fits both the experimental amplitude ratio and phase lag finding. The goodness of fit of the postulated model could be confirmed by statistical analysis.

The intent of this work is not to develop complex, definitive models, but rather to investigate the feasibility of modeling a test system by a simple network of ideal reactors.

The postulated models are therefore purposely limited to simple series configurations composed of two ideal reactor types, namely completely mixed tanks and plug flow reactors. An allowance for dead space is also included in some models.

The purpose served by these models is not that they provide an exact description of the experimental system but rather that they illustrate several facets of the use of Bode plot representations of frequency response data in developing models.

In the writer's opinion, one of the main advantages offered by this type of analysis is that an overall understanding of a particular system can be gained directly from a Bode plot representation of test data. From the slope of the amplitude plot an insight can be gained into the number of CSTR's in the system. A simple graphical approximation of the amplitude curve provides further information concerning the size of the completely mixed segments. Knowing the number and approximate size of the CSTR components, the phase lag curve can be used to determine the presence and approximate size of any PFR in the system. The result is that an understanding of the test system is realized directly from the experimental data.

To accurately model a test system, a wider range of frequencies should be used to gather more data points to define the system's phase lag and amplitude ratio curves. The precision of the experimental data could be enhanced by refining the monitoring equipment to provide an "in situ" measurement of both the input and the output sine waves. In this way, the response lag associated with fluorometric monitoring could be eliminated and the test results would then be

truly representative of the system under study. From the experimental data the initial model assumption could then be made in much the same manner as is done in this work and subsequently, an iterative, computerized search technique could be employed to find the model bearing the best correlation with the test system. No doubt, much more complex models consisting of parallel as well as series configurations would be required to describe a system with statistical confidence.

Having developed a model in this manner, it would then be necessary to determine the relative placement of the various components in the overall model configuration. It should be possible to do this by measuring the conversion that takes place when a substance with a known reaction mechanism is introduced into the test system. To differentiate between the placement of CSTR and PFTR components in the network, a non-linear reaction mechanism should be used.

CHAPTER 7

CONCLUSIONS AND RECOMMENDATIONSCONCLUSIONS

As a result of this investigation, it can be concluded that:

1. It is possible to produce and monitor sine wave disturbances to gather frequency response data from laboratory flow through vessels. This technique should therefore also be applicable to field scale studies.
2. The feasibility of modeling a test system using networks of ideal hydraulic components has been demonstrated.
3. Frequency response testing and analysis is an advantageous method of studying the dynamic hydraulic characteristics of reaction vessels. One of the major merits of this technique is that conventional Bode plot representations of experimental data greatly facilitate and provide flexibility in modeling.

RECOMMENDATIONS

Further studies should be undertaken over a wider range of test frequencies and with refined monitoring equipment to gather data from a more complex laboratory model or an actual field installation reactor. In combination with this, a computerized search technique could be investigated as a means

of accurately modeling the experimental system with a network of ideal hydraulic components. As a final step in model definition, the test system response to a known reaction mechanism could be measured and compared to the theoretical response from the chosen model.

REFERENCES

- (1) ADLER, R.J., "Finite Stage Modelling", 4th Nat. Chem. & Petroleum Symposium of the Instrument Society of America, (1962).
- (2) BODE, H.W., "Network Analysis and Feedback Amplifier Design", D. Van Nostrand Co., Inc., Princeton, N.J., (1945).
- (3) CLEMENTS, Jr., W.C., and SCHNELLE, Jr., K.B., "Pulse Testing for Dynamic Analysis", I & EC Process Design and Development, II, 2, April, (1963).
- (4) COLUCCI, F.W., Jr., "pH Control of a Continuous Neutralization in a Stirred Tank", M.S. thesis, as cited in Harriott, P., "Process Control", p.344.
- (5) COUGHANOWR, D.R., and KOPPEL, L.B., "Process Systems Analysis and Control", McGraw-Hill, (1965).
- (6) DANCKWERTZ, P.V., "Continuous Flow Systems - Distribution of Residence Times", Chemical Engineering Science, 2, 1, (1953).
- (7) FEUERSTEIN, D.L., and SELLECK, R.E., "Fluorescent Tracers for Dispersion Measurements", Proc. A.S.C.E., Journal of Sanitary Engineering Division, 89, SA4, 2, (1963).
- (8) GEERLINGS, M.W., "Plant and Process Dynamic Characteristics", Academic Press, New York, (1957).
- (9) HARRIOTT, P., "Process Control", McGraw-Hill, New York, (1964).
- (10) HOUGEN, J.O., and WALSH, R.A., "Pulse Testing Method", Chem. Eng. Progress, 57, 3, March, (1961).
- (11) KEHR, R.W., "Detention of Liquids Being Mixed in Continuous Flow Tanks", Sewage Works Journal, 8, 915, (1936).
- (12) KESSMER, H.J.N.H., "Annual Report, Government Institute for Purification of Waste Waters, 1933", Sewage Works Journal, 7, 135, (1935).

- (13) KRAMERS, H., and ALBERDA, G., "Frequency response analysis of continuous flow systems", Chem. Eng. Sci., Vol. 12, 173, (1953).
- (14) KRAMERS, H., "The Dynamic Behavior of Processes, in Particular for pH Control", Trans. Soc. Instr. Technol., 8, 144, (1956).
- (15) LEES, S., and HOUGEN, J.O., Ind. Eng. Chem., 48, 1058, (1956), as cited in Hougen, J.O., and Walsh, R.A., "Pulse Testing Method", Chem. Eng. Progress, 57, 3, March, (1961).
- (16) LEVENSPIEL, O., "Chemical Reaction Engineering", Wiley, New York, (1962).
- (17) LEVENSPIEL, O., "Comparison of the Tank-in-series and Dispersion Models for Non-ideal Flow of Fluid", Chem. Eng. Sci., 17, 576, (1962).
- (18) LEVENSPIEL, O., and SMITH, W.K., "Notes on the Diffusion-type Model for Longitudinal Mixing of Fluids in Flow", Chem. Eng. Sci., 6, 227, (1957).
- (19) LYNCH, W.A., and TRUXAL, J.G., "Introductory System Analysis", McGraw-Hill, New York, (1961).
- (20) MURRILL, P.W., "Automatic Control of Process", International Textbook Co., Scranton, Pa., (1967).
- (21) MURRILL, P.W., PIKE, R.W., and SMITH, C.L., "Development of Dynamic Mathematical Models", Chem. Eng., September 9, 117, (1968).
- (22) MURRILL, P.W., PIKE, R.W., and SMITH, C.L., "Frequency Response Data Yield Analytic Equations", Chem. Eng., November 18, 165, (1968).
- (23) MURRILL, P.W., PIKE, R.W., and SMITH, C.L., "Pulse Testing Methods", Chem. Eng., February 24, 105, (1969).
- (24) MURRILL, P.W., PIKE, R.W., and SMITH, C.L., "The Basis for Bode Plots", Chem. Eng., October 7, 177, (1968).
- (25) MURRILL, P.W., PIKE, R.W., and SMITH, C.L., "Transient Response in Dynamic-Systems Analyses", Chem. Eng., December 16, 103, (1968).

- (26) MURRILL, P.W., PIKE, R.W., and SMITH, C.L., "Pulse Testing Methods", Chem. Eng., February 24, 105, (1969).
- (27) PERLMUTTER, D.D., "Introduction to Chemical Process Control", John Wiley & Sons, Inc., New York, (1965).
- (28) PIPES, W.O., et al, "A Laboratory Study of Mixing Conditions in Small Aeration Vessels", 19th Ind. Waste Conf., Purdue University, 927, (1964).
- (29) PIPES, W.O., et al, "Compartmentalization of Aeration Tanks", Proc. A.S.C.E., Journal of the Sanitary Engineering Division, 91, Sa3, 45, (1965).
- (30) ROOZE, J.W., "Determination of Residence Time Distribution Using Deterministic and Random Signals", M.Sc. Thesis, as cited in MELNYK, P.B., "The Representation of the Non-ideal Mixing in a Flow Reactor by a Network of Idealized Components", M. Eng. Thesis, McMaster University, (1970).
- (31) TEASDALE, JR., A.R., "Frequency Response From Transient Data", as cited in Murrill et al, "Transient-Response Data Yield Frequency-Response Models".
- (32) TIMPANY, P.L. "Variations of Axial Mixing in an Aeration Tank", M.Eng. Thesis, Civil Eng., McMaster University, (1966).
- (33) THOMAS, H.A., and McKEE, J.E., "Longitudinal Mixing in Aeration Tanks", Sewage Works Journal, 16, 42, (1944).
- (34) WILHELM, R.H., "Rate Process in Chemical Reactors", Chem. Eng. Progress, March, 49, 3, (1953).

APPENDIX NUMBER I

INPUT SINE WAVE CHARACTERISTICS

INPUT WAVE - PROOF OF SINUSOIDAL NATURE

The input waveform generating equipment can be represented as shown in Figure 13.

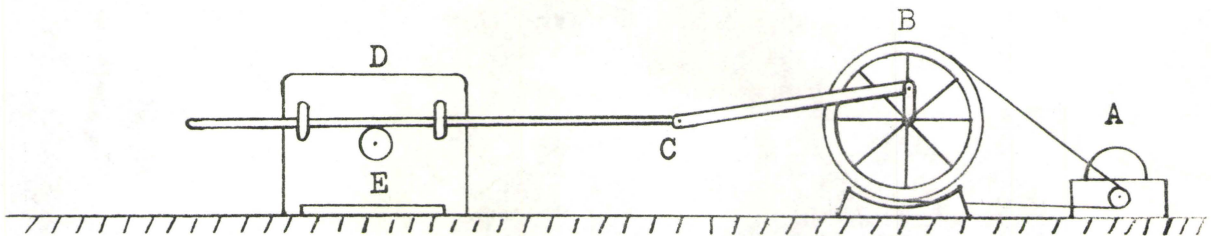
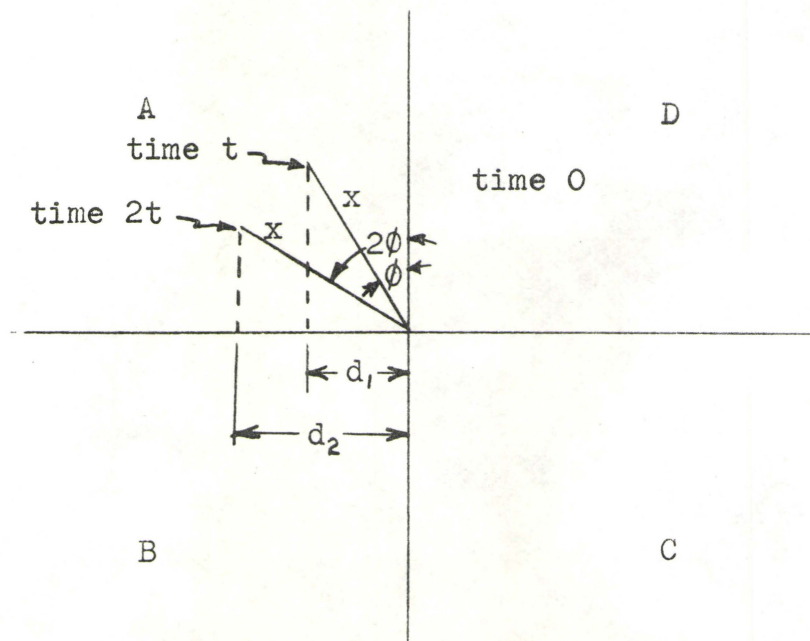


FIGURE 13

- A = electric motor - gear reducer unit
- B = 12 inch pulley with fixed driving arm attached to shaft
- C = push rod and gear rack assembly
- D = kinetic clamp pump
- E = spur gear driving circular rheostat

The gear reducer unit imparts a constant angular momentum to the 12 inch pulley and so to the driving arm fixed to the pulley shaft. Therefore, for each increment of time Δt , the position of the drive rod is changed by an angle $\Delta\phi$. This can be shown in the following manner:



Now to prove that the input is a sine wave, the horizontal displacement of the gear rack with time is of interest. To study this, assume the length of the driving arm is x and its projection on the horizontal axis is d_1, d_2, \dots, d_n at equal increments of time $t, 2t, \dots, nt$ respectively. Now relating all horizontal displacement to the origin or the centre of the drive shaft, with displacement to the right being negative and displacement to the left positive, then the following relations between t, ϕ , and d are found.

In quadrant A where $n\phi \leq 90^\circ$

$$\begin{aligned} \text{at time } t \dots d_1 &= x \sin \phi \\ \text{at time } 2t \dots d_2 &= x \sin 2\phi \\ \text{at time } nt \dots d_n &= x \sin n\phi \end{aligned}$$

Similarly in quadrant B where $180^\circ \leq n\phi < 90^\circ$

$$\text{at time } nt \dots d_n = x \sin (-n\phi + 180^\circ)$$

In quadrant C where $270^\circ \leq n\phi < 180^\circ$

$$\text{at time } nt \dots d_n = -x \sin (n\phi - 180^\circ)$$

And in quadrant D where $360^\circ \leq n\phi < 270^\circ$

$$\text{at time } nt \dots d_n = -x \sin (360^\circ - n\phi)$$

Therefore it is evident that since x is a constant, the horizontal displacement with time varies in a sinusoidal manner.

For the sake of clarity and as an example of a typical input, consider the case where $x = 1.5$ inches and a complete cycle is generated in 360 seconds. In this case each second corresponds to 1 degree change in the angular position of the drive arm. Calculating the input for 15 second time intervals

starting from 0 when the drive arm is coincident with the positive vertical axis yields:

TABLE I-1

<u>TIME</u> <u>(seconds)</u>	<u>ANGULAR</u> <u>DISPLACEMENT</u> <u>(ϕ in degrees)</u>	<u>SINE ϕ</u>	<u>HORIZONTAL</u> <u>DISPLACEMENT</u> <u>(inches)</u>
0	0	0.000	0.00
15	15	0.259	0.39
30	30	0.500	0.75
45	45	0.707	1.06
60	60	0.866	1.30
75	75	0.966	1.45
90	90	1.000	1.50
105	105	0.966	1.45
120	120	0.866	1.30
135	135	0.707	1.06
150	150	0.500	0.75
165	165	0.259	0.39
180	180	0.000	0.00
195	195	-0.259	-0.39
210	210	-0.500	-0.75
225	225	-0.707	-1.06
240	240	-0.866	-1.30
255	255	-0.966	-1.45
270	270	-1.000	-1.50
285	285	-0.966	-1.45
300	300	-0.866	-1.30
315	315	-0.707	-1.06
330	330	-0.500	-0.75
345	345	-0.259	-0.39
360	360	0.000	0.00

Knowing that the horizontal movement of the gear rack varied sinusoidally and knowing that tracer flow rate varied linearly with the rheostat setting of the kinetic clamp pump then it can be concluded that the input tracer concentration varied sinusoidally.

CALCULATION OF INPUT SINE WAVE AMPLITUDES

In all experimental tests the maximum and minimum rates of pumpage for the kinetic clamp pump were 82% and 20% of full flow respectively.

From the calibration curve for the kinetic clamp pump
(Appendix IV)

82% full flow = 0.67 milliliters/second
20% full flow = 0.16 milliliters/second
(average) 51% full flow = 0.41 milliliters/second

Experiment Number I

feed concentration = 0.072 mg Rhodamine B / ml
fluid flow rate = 424 ml/second

Therefore: sine wave peak = 113.9 ppb
sine wave low = 26.7 ppb
average concentration = 70.3 ppb
sine wave amplitude = 43.6 ppb

Experiment Number II

Similarly with the same feed concentration and a fluid flow of 206 ml/second , the input sine wave amplitude is 89.7 ppb.

Experiment Number III

A feed concentration of 0.084 mg/ml coupled with a carrier fluid flow rate of 428 ml/sec yields an input sine wave amplitude of 50.4 ppb.

Experiment Number IV

The same conditions as in Experiment Number I yield an input sine wave amplitude of 43.6 ppb.

APPENDIX NUMBER II

EXPERIMENTAL DATA

EXPERIMENT NUMBER I

Date: September 24, 1968

Tank Dimensions - Width = 19.4 centimeters
 - Length = 97.5 centimeters
 - Liquid depth = 13.3 centimeters

Tank Volume = 25,160 cubic centimeters

Flow Rate = 424 cubic centimeters per second

Theoretical detention time = 59.3 seconds

Input Sine Wave - peak = 113.9 ppb = 2.63 millivolts
 - low = 26.7 ppb = 0.40 millivolts
 (refer to fluorometer calibration curve A)

Input Amplitude = 43.6 ppb

TABLE II-1

TEST NUMBER I				MIXER OFF				
Run Number	A	B	C	D	E	F	G	H
Sine Wave Peak	(mv)	2.35	2.55	2.38	1.98	1.86	1.70	1.57
	(ppb)	102.9	110.9	104.1	88.7	83.7	77.8	72.5
Sine Wave Low	(mv)	0.72	0.47	0.56	0.97	1.11	1.24	1.31
	(ppb)	39.4	29.7	33.3	49.2	54.5	59.6	62.3
Amplitude (ppb)	31.8	40.6	35.4	19.8	14.6	9.1	5.1	
Amplitude Ratio	0.73	0.93	0.81	0.45	0.33	0.21	0.12	
Sine Wave Period (sec)	222	449	397	120	91.5	64	34	
Sine Wave Frequency (radians/second)	0.028	0.014	0.0159	0.0524	0.0686	0.0988	0.185	
- seconds	54	54	60	42	38	33	24	
Phase Angle - radians	1.51	0.756	0.95	2.20	2.61	3.26	4.52	
- degrees	87	43	55	126	150	187	259	

EXPERIMENT NUMBER I

Date: September 24, 1968

Tank Dimensions - Width = 19.4 centimeters
 - Length = 97.5 centimeters
 - Liquid depth = 13.3 centimeters

Tank Volume = 25,160 cubic centimeters

Flow Rate = 424 cubic centimeters per second

Theoretical detention time = 59.3 seconds

Input Sine Wave - peak = 113.9 ppb = 2.63 millivolts
 - low = 26.7 ppb = 0.40 millivolts
 (refer to fluorometer calibration curve A)

Input Amplitude = 43.6 ppb

TABLE II-2

TEST NUMBER II				MIXER ON				
Run Number	A	B	C	D	E	F	G	H
Sine Wave Peak	(mv)	2.35	2.50	2.36	1.95	1.87	1.74	1.61
	(ppb)	102.8	108.8	103.4	87.5	84.1	79.2	74.2
Sine Wave Low	(mv)	0.65	0.53	0.65	1.07	1.14	1.26	1.39
	(ppb)	36.4	31.9	36.7	53.0	55.9	60.4	65.6
Amplitude (ppb)	33.2	38.4	33.3	17.3	14.1	9.4	4.3	
Amplitude Ratio	0.76	0.88	0.76	0.40	0.32	0.22	0.10	
Sine Wave Period (sec)	222	449	397	120	91.5	64	34	
Sine Wave Frequency (radians/second)	0.028	0.014	.0159	.0524	.0686	.0988	0.185	
Phase Angle	-seconds	48	51	52	42	36	33	25
	-radians	1.34	0.71	0.83	2.20	2.47	3.26	4.63
	-degrees	77	41	48	126	142	187	265

EXPERIMENT NUMBER II

Date: September 26, 1968

Tank Dimensions - Width = 19.4 centimeters
 - Length = 97.5 centimeters
 - Liquid depth = 12.4 centimeters

Tank Volume = 23,350 cubic centimeters

Flow Rate = 206 cubic centimeters per second

Theoretical detention time = 113.5 seconds

Input Sine Wave - peak = 234.1 ppb = 5.12 millivolts
 - low = 54.8 ppb = 1.24 millivolts
 (refer to calibration curve B)

Input Amplitude = 89.7 ppb

TABLE II-3

TEST NUMBER I				MIXER OFF				
Run Number	A	B	C	D	E	F	G	H
Sine Wave Peak	(mv)	4.19	4.84	4.68	4.55	4.12	3.74	3.54
	(ppb)	192.8	221.6	214.6	208.7	189.9	172.9	164.1
Sine Wave Low	(mv)	2.02	1.40	1.66	1.71	2.14	2.48	2.71
	(ppb)	97.1	69.6	81.0	83.3	102.5	117.3	127.5
Amplitude (ppb)	47.9	76.0	66.3	62.7	43.7	27.8	18.3	
Sine Wave Period(sec)	229	468	351	303	207	146	104	
Amplitude Ratio	0.55	0.87	0.76	0.72	0.50	0.32	0.21	
Sine Wave Frequency (radians/second)	.0274	.0134	.0179	.0207	.0303	.0430	.0606	
- seconds	87	114	106.5	120	105	84	72	
Phase Angle - radians	2.38	1.53	1.91	2.48	3.18	3.61	4.36	
- degrees	136	88	109	142	182	207	250	

Date: September 26, 1968

Tank Dimensions - Width = 19.4 centimeters
 - Length = 97.5 centimeters
 - Liquid depth = 12.4 centimeters

Tank Volume = 23,350 cubic centimeters

Flow Rate = 206 cubic centimeters per second

Theoretical detention time = 113.5 seconds

Input Sine Wave - peak = 234.1 ppb = 5.12 millivolts
 - low = 54.8 ppb = 1.24 millivolts
 (refer to fluorometer calibration curve B)

Input Amplitude = 89.7 ppb

TABLE II-4

TEST NUMBER II				MIXER ON				
Run Number	A	B	C	D	E	F	G	H
Sine Wave Peak	(mv)	3.93	4.51	4.31	4.16	3.86	3.64	3.48
	(ppb)	181.9	207.4	198.6	192.0	178.6	168.9	161.9
Sine Wave Low	(mv)	2.20	1.71	1.91	2.04	2.31	2.55	2.69
	(ppb)	105.2	83.3	92.4	97.9	109.9	120.6	126.7
Amplitude (ppb)	38.3	61.8	53.1	47.0	34.4	24.2	17.6	
Amplitude Ratio	0.42	0.69	0.59	0.52	0.38	0.27	0.20	
Sine Wave Period (sec)	229	468	351	303	207	146	104	
Sine Wave Frequency (radians/second)	.0274	.0134	.0179	.0207	.0303	.0430	.0606	
- seconds	53	99	78	75	68	54	48	
Phase Angle	- radians	1.45	1.33	1.40	1.55	2.05	2.32	2.91
	- degrees	83	76	80	89	117	133	167

Date: September 27, 1968

Tank Dimensions - Width = 19.4 centimeters
 - Length = 193.5 centimeters
 - Liquid Depth = 12.5 centimeters

Tank Volume = 47,700 cubic centimeters

Flow Rate = 428 cubic centimeters per second

Theoretical Detention time = 109 seconds

Input Sine Wave - peak = 131.7 ppb = 2.92 millivolts
 - low = 30.8 ppb = .54 millivolts
 (refer to fluorometer calibration curve C)

Input Amplitude = 50.4 ppb

TABLE II-5

TEST NUMBER I		MIXER OFF							
Run Number		A	B	C	D	E	F	G	H
Sine Wave Peak	(mv)	2.78	2.58	2.75	2.92	2.69	2.57	2.22	2.00
	(ppb)	125.6	117.3	124.4	131.4	122.0	116.9	101.9	92.4
Sine Wave Low	(mv)	0.56	0.82	0.65	0.54	0.75	0.93	1.25	1.49
	(ppb)	31.4	42.6	35.3	30.7	39.7	47.0	60.7	71.0
Amplitude (ppb)		47.1	37.3	44.6	50.3	41.2	35.0	20.6	10.7
Amplitude Ratio		0.93	0.74	0.88	.998	0.82	0.69	0.41	0.21
Sine Wave Period (sec)		860	218	296	492	200	153	88	64
Sine Wave Frequency (radians/second)		.0073	.0288	.0212	.0128	.0134	.041	.071	.099
Phase Angle	-seconds	120	96	102	90	96	98	90	90
	-radians	.877	2.76	2.16	1.152	3.01	4.02	6.39	8.91
	-degrees	50	158	124	66	172	230	366	510

Date: October 3, 1968

Tank Dimensions - Width = 19.4 centimeters
 - Length = 48.7 centimeters
 - Liquid Depth = 13.8 centimeters

Tank Volume = 13,000 cubic centimeters

Flow Rate = 424 cubic centimeters per second

Theoretical detention time = 30.8 seconds

Input Sine Wave - peak = 113.9 ppb = 3.13 millivolts
 - low = 26.7 ppb = 0.55 millivolts
 (refer to fluorometer calibration curve D)

Input Amplitude = 43.6 ppb

TABLE II-6

TEST NUMBER I				MIXER OFF					
Run Number	A	B	C	D	E				
Sine Wave Peak	(mv)	2.31	2.41	2.52	2.60	2.85			
	(ppb)	86.2	89.6	93.0	96.0	104.5			
Sine Wave Low	(mv)	1.40	1.29	1.18	1.12	0.85			
	(ppb)	55.4	51.7	48.0	46.0	37.5			
Amplitude (ppb)	15.4	18.9	22.5	25.0	33.5				
Amplitude Ratio	0.35	0.43	0.52	0.57	0.77				
Sine Wave Period(sec)	17.5	25	47	77	137				
Sine Wave Frequency (radians/second)	0.36	0.25	.134	.082	.046				
Phase Angle	- seconds	8.5	-	-	15	24			
	- radians	3.06	-	-	1.23	1.10			
	- degrees	175	-	-	71	63			

APPENDIX NUMBER III

OUTPUT SINE WAVE CHARACTERISTICS

COMPARISON OF OUTPUT SIGNALS TO SINE FUNCTION

Input Sine Wave = $R = R_o \sin wt$

Output Sine Wave = $C = C_o \sin (wt + \phi)$

Where R_o = input sine wave amplitude (millivolts)
 C_o = output sine wave amplitude (millivolts)
 ϕ = degrees of phase shift (negative angle)
 w = frequency (radians per second)
 t = time (seconds)

TABLE III-1EXPERIMENT I TEST II RUN B

$R_o = 1.11$ mv
 $C_o = 0.99$ mv

$\phi = -.71$ radians = -40.7 degrees
 $w = .014$ radians/second

Time "t" seconds	wt degrees	wt + ϕ degrees	Input Sine Wave Value R	Output Sine Wave Value C	
				actual	theoretical
0	0	-40.7	0.0	---	---
30	24.1	-16.6	0.45	---	---
60	48.1	7.4	0.83	0.12	0.13
90	72.2	31.5	1.06	0.50	0.52
120	96.3	55.6	1.10	0.78	0.82
150	120.3	79.6	0.96	0.95	0.97
180	144.4	103.7	0.65	0.97	0.96
210	168.5	127.8	0.22	0.80	0.78
240	192.5	151.8	-0.24	0.50	0.47
270	216.6	175.9	-0.66	0.10	0.07
300	240.7	200.0	-0.97	-0.30	-0.34
330	264.7	224.0	-1.11	-0.64	-0.69
360	288.8	248.1	-1.05	-0.89	-0.92
390	312.9	272.2	-0.81	-0.96	-0.99
420	336.9	296.2	-0.44	-0.85	-0.89
450	361.0	320.3	0.02	-0.63	-0.63
480	385.1	344.4	0.47	-0.25	-0.27
510	409.1	368.4	0.84	0.15	0.14
540	433.2	392.5	1.06	0.51	0.53

EXPERIMENT I TEST I RUN C

$$R_o = 1.11\text{mv} \quad \& = -.954 \text{ radians} = -54.6 \text{ degrees}$$

$$C_o = 0.91\text{mv} \quad w = .0159 \text{ radians/second}$$

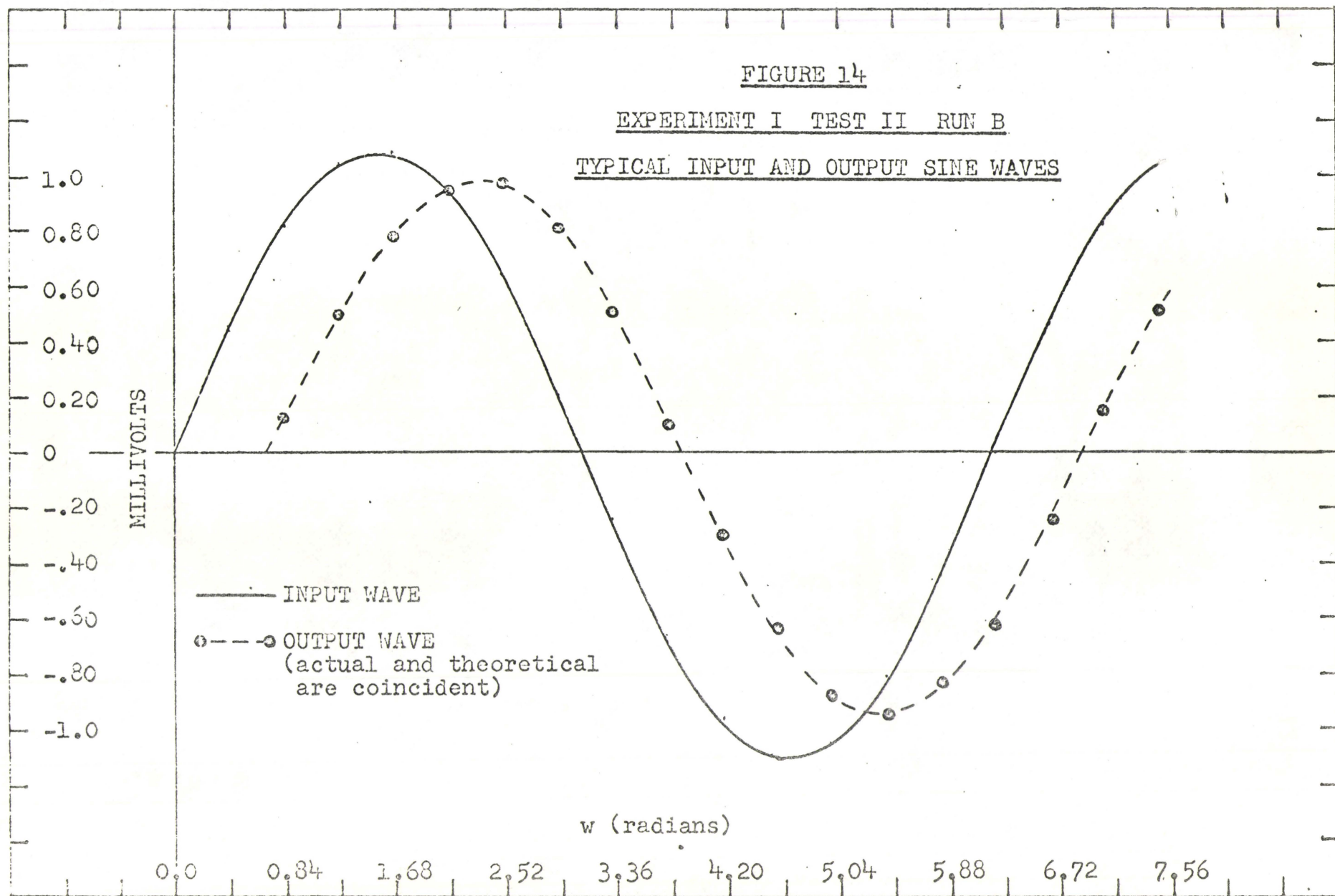
TABLE III-2

Time "t" seconds	wt degrees	wt + & degrees	Input Sine Wave Value R	Output Sine Wave Value C	
				actual	theoretical
0	0.0	-54.6	0.0	---	---
30	27.3	-27.3	0.51	---	---
60	54.7	0.0	0.91	0.0	0.0
90	82.0	27.3	1.10	0.43	0.42
120	109.3	54.7	1.05	0.77	0.74
150	136.7	82.0	0.76	0.88	0.90
180	164.0	109.3	0.31	0.83	0.86
210	191.3	136.7	-0.22	0.58	0.62
240	218.7	164.0	-0.69	0.21	0.25
270	246.0	191.3	-1.01	-0.22	-0.18
300	273.3	218.7	-1.08	-0.62	-0.57
330	300.7	246.0	-0.95	-0.82	-0.83
360	328.0	273.3	-0.59	-0.87	-0.88
390	355.3	300.7	-0.09	-0.75	-0.78
420	382.7	328.0	0.43	-0.45	-0.48
450	410.0	355.3	0.85	-0.05	-0.07
480	437.3	382.7	1.08	0.38	0.35

FIGURE 14

EXPERIMENT I TEST II RUN B

TYPICAL INPUT AND OUTPUT SINE WAVES



EXPERIMENT II TEST I RUN D

$$R_o = 1.94 \text{ mv} \quad \phi = -2.48 \text{ radians} = -142^\circ$$

$$C_o = 1.42 \text{ mv} \quad \omega = .0207 \text{ radians/second}$$

TABLE III-3

Time "t" seconds	wt degrees	wt + ϕ degrees	Input Sine Wave Value R	Output Sine Wave Value C	
				actual	theoretical
0	0.0	-142.1	0.0	---	---
30	35.5	-106.6	1.13	---	---
60	71.1	-71.1	1.84	---	---
90	106.6	-35.5	1.86	---	---
120	142.1	0.0	1.19	0.0	0.0
150	178.2	35.5	0.06	0.80	0.83
180	213.7	71.1	-1.08	1.33	1.34
210	249.3	106.6	-1.81	1.37	1.36
240	284.8	142.1	-1.88	0.90	0.87
270	320.3	178.2	-1.24	0.02	0.04
300	355.8	213.7	-0.14	-0.81	-0.79
330	391.4	249.3	1.01	-1.32	-1.33
360	426.9	284.8	1.78	-1.34	-1.37
390	462.4	320.3	1.90	-0.86	-0.90
420	497.9	355.8	1.30	-0.06	-0.10
450	434.0	391.4	0.20	0.75	0.74
480	969.6	426.9	-0.96	1.35	1.31

$$R_0 = 1.94 \text{ mv} \quad \phi = -1.55 \text{ radians} = -89^\circ$$

$$C_0 = 1.06 \text{ mv} \quad \omega = .0207 \text{ radians/second}$$

TABLE III-4

Time "t" seconds	wt degrees	wt + ϕ degrees	Input Sine Wave Value R	Output Sine Wave Value C	
				actual	theoretical
0	0.0	-88.3	0.0	---	---
30	35.5	-53.3	1.13	---	---
60	71.1	-17.8	1.84	---	---
90	106.6	17.8	1.86	0.30	0.32
120	142.1	53.3	1.19	0.85	0.85
150	178.2	89.4	0.06	1.05	1.06
180	213.7	124.9	-1.08	0.90	0.87
210	249.3	160.4	-1.81	0.40	0.36
240	284.8	196.0	-1.88	-0.25	-0.29
270	320.3	231.5	-1.24	-0.83	-0.83
300	355.8	267.0	-0.14	-1.05	-1.06
330	391.4	302.5	1.01	-0.87	-0.89
360	426.9	338.1	1.78	-0.40	-0.40
390	462.4	373.6	1.90	0.27	0.25
420	497.9	409.1	1.30	0.80	0.80

EXPERIMENT III TEST I RUN A

$$R_o = 1.19 \text{ mv} \quad \& = -0.877 \text{ radians} = -50^\circ$$

$$C_o = 1.11 \text{ mv} \quad w = .0073 \text{ radians/second}$$

TABLE III-5

Time "t" seconds	wt degrees	wt + & degrees	Input Sine Wave Value R	Output Sine Wave Value C	
				actual	theoretical
0	0.0	-50.3	0.0	---	---
60	25.2	-25.2	0.51	---	---
120	50.4	0.0	0.92	0.0	0.0
180	75.1	25.2	1.15	0.50	0.47
240	100.3	50.4	1.17	0.75	0.86
300	125.5	75.1	0.97	0.90	1.07
360	150.7	100.3	0.58	1.05	1.09
420	175.9	125.5	0.09	1.00	0.90
480	200.6	150.7	-0.42	0.70	0.54
540	225.8	175.9	-0.85	0.20	0.08
600	251.0	200.6	-1.13	-0.30	-0.39
660	276.2	225.8	-1.18	-0.70	-0.80
720	301.4	251.0	-1.02	-0.90	-1.05
780	326.0	276.2	-0.67	-1.05	-1.10
840	351.2	301.4	-0.18	-1.00	-0.95
900	376.5	326.0	0.34	-0.70	-0.62
960	401.7	351.2	0.79	-0.20	-0.17
1021	426.9	376.5	1.09	0.20	0.32
1080	451.5	401.7	1.19	0.40	0.74

EXPERIMENT III TEST I RUN C

$$R_0 = 1.19 \text{ mv} \quad \& = -2.16 \text{ radians} = -124^\circ$$

$$C_0 = 1.05 \text{ mv} \quad w = .0212 \text{ radians/second}$$

TABLE III-6

Time "t" seconds	wt degrees	wt + & degrees	Input Sine Wave Value R	Output Sine Wave Value C	
				actual	theoretical
0	0.0	-123.8	0.0	---	---
30	36.7	- 87.1	0.71	---	---
60	72.8	- 51.0	1.14	---	---
90	109.4	- 14.3	1.12	---	---
120	145.5	21.8	0.67	0.35	0.39
150	182.2	58.4	-0.05	0.85	0.89
180	218.9	95.1	-0.75	1.03	1.05
210	255.0	131.2	-1.15	0.73	0.79
240	291.7	167.9	-1.11	0.30	0.22
270	327.8	204.0	-0.63	-0.45	-0.43
300	364.4	240.7	0.09	-0.90	-0.92
330	400.5	276.8	0.77	-1.02	-1.04
360	437.2	313.4	1.16	-0.75	-0.76
390	473.9	350.1	0.48	-0.20	-0.18
420	510.0	386.2	0.60	0.45	0.46

EXPERIMENT IV TEST I RUN E

$$R_o = 1.29 \text{ mv} \quad \& = -1.10 \text{ radians} = -63^\circ$$

$$C_o = 1.00 \text{ mv} \quad w = .046 \text{ radians/second}$$

TABLE III-7

Time "t" seconds	wt degrees	wt + & degrees	Input Sine Wave Value R	Output Sine Wave Value C	
				actual	theoretical
0	0.0	-63.0	0.0	---	---
15	39.5	-23.5	0.82	---	---
30	79.1	16.0	1.27	0.27	0.28
45	118.6	55.6	1.13	0.62	0.83
60	158.1	95.1	0.48	0.62	0.99
75	197.7	134.7	-0.39	0.68	0.71
90	237.2	174.2	-1.08	0.20	0.10
105	276.8	213.7	-1.28	-0.38	-0.56
120	316.3	253.3	-0.89	-0.82	-0.96
135	355.8	292.8	-0.09	-0.92	-0.92
150	395.4	332.3	0.75	-0.55	-0.47
165	434.9	371.9	1.24	-0.08	-0.21

APPENDIX NUMBER IV

FLUOROMETER AND KINETIC CLAMP PUMP

CALIBRATION CURVES

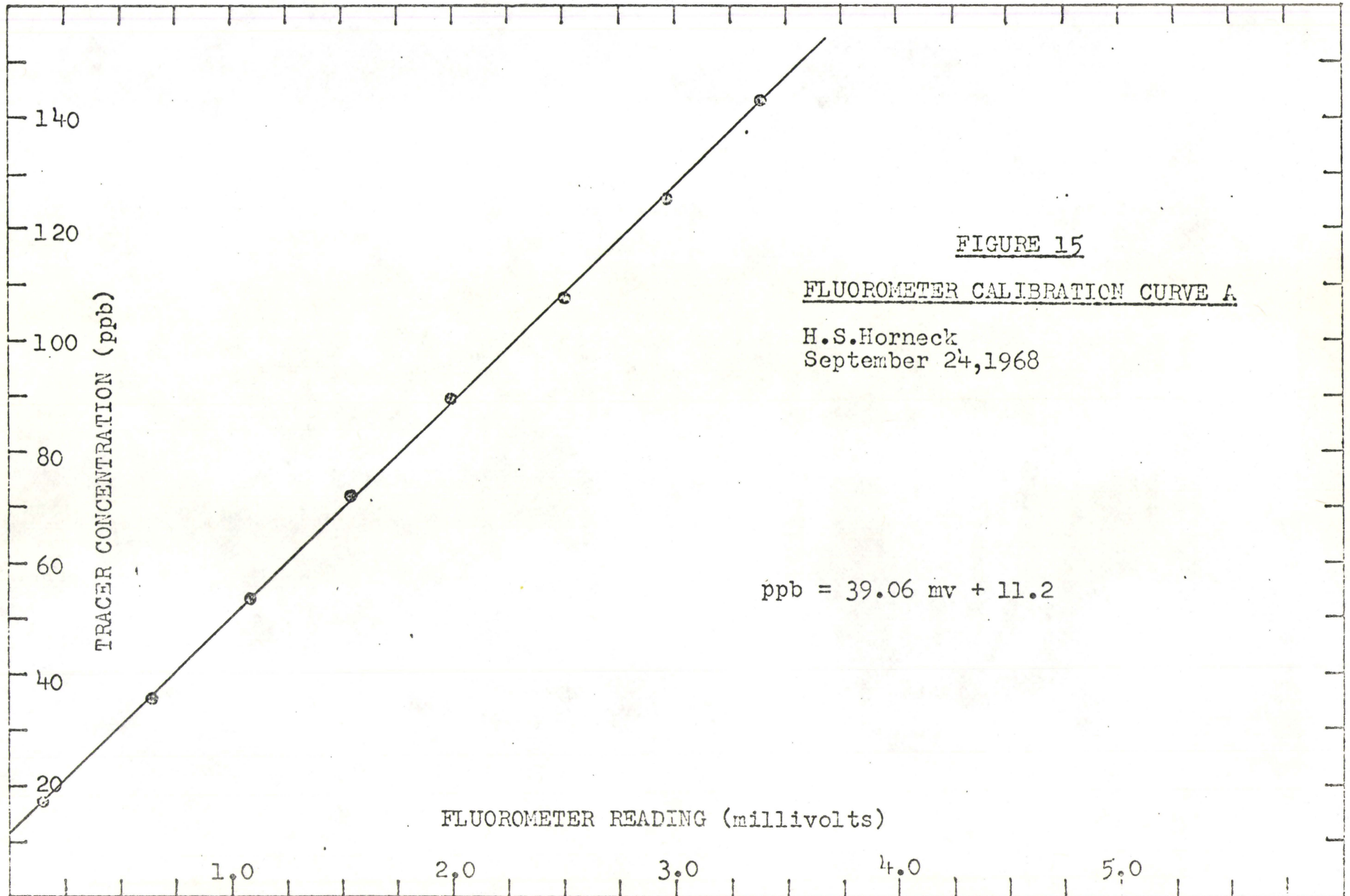


FIGURE 15

FLUOROMETER CALIBRATION CURVE A

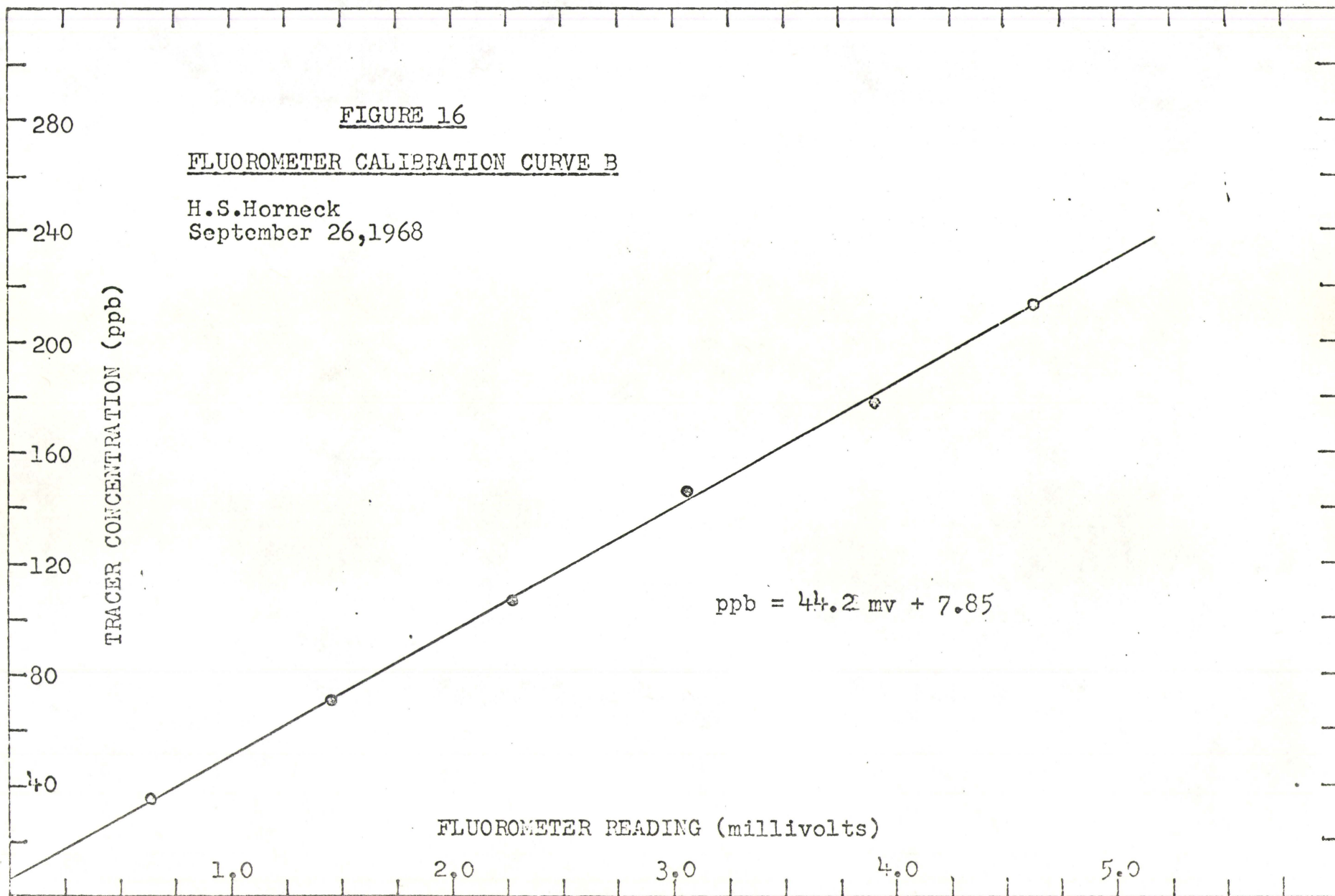
H.S.Horneck
September 24, 1968

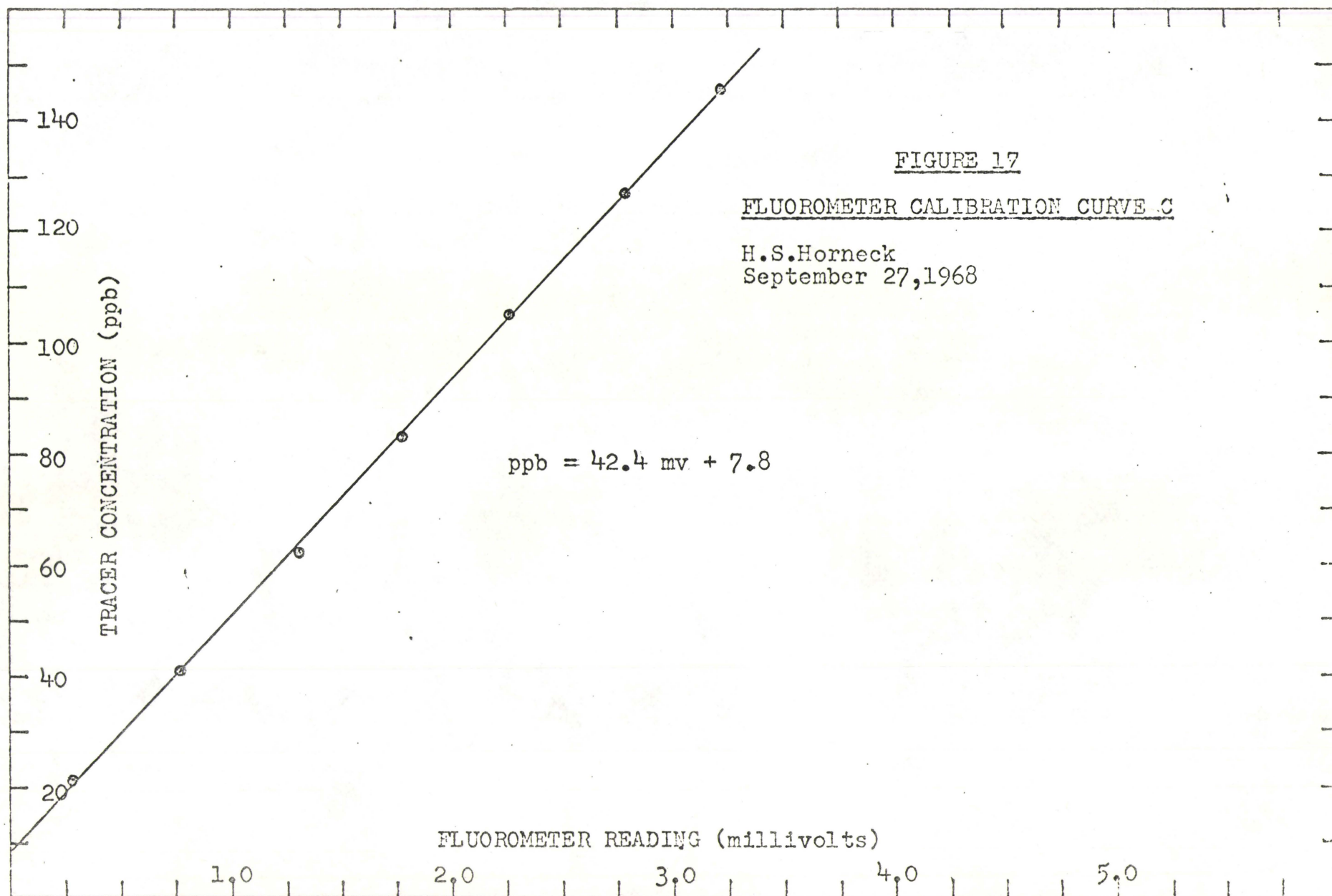
$$\text{ppb} = 39.06 \text{ mv} + 11.2$$

FIGURE 16

FLUOROMETER CALIBRATION CURVE B

H.S.Horneck
September 26, 1968





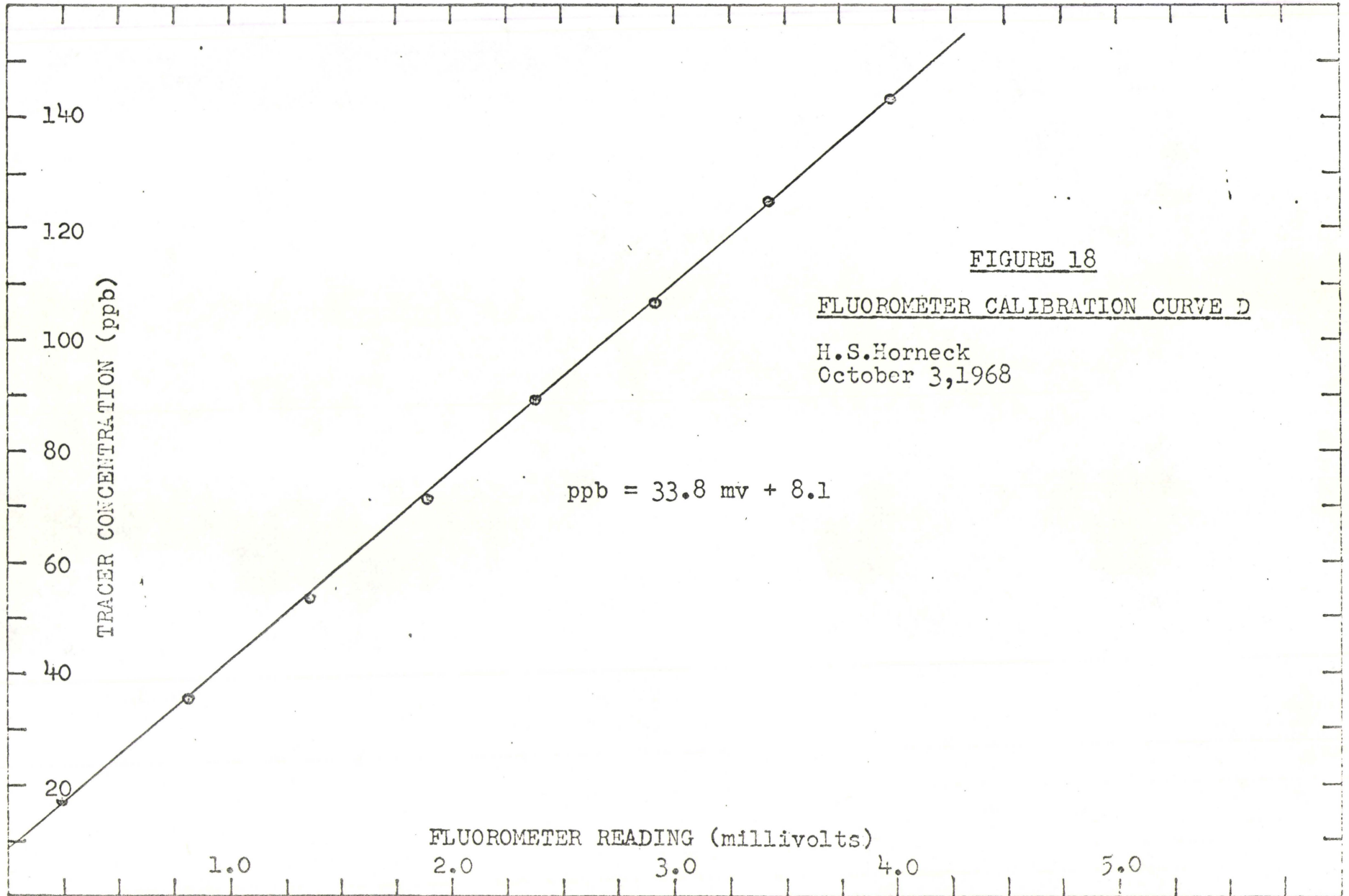


FIGURE 18

FLUOROMETER CALIBRATION CURVE D

H.S.Horneck
October 3, 1968

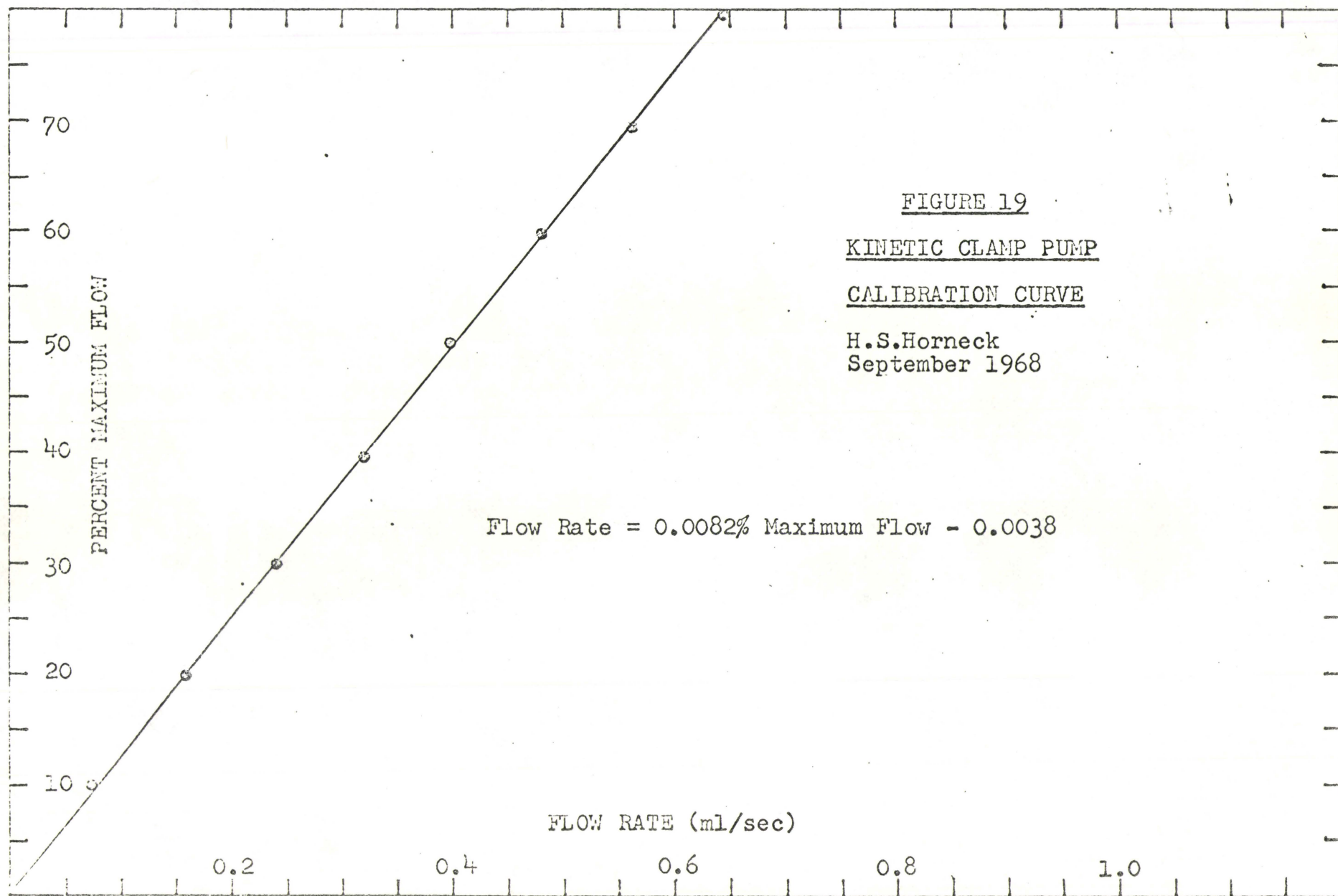


FIGURE 19
KINETIC CLAMP PUMP
CALIBRATION CURVE

H.S.Horneck
September 1968

APPENDIX V

MODELING

TABLE V-1MODELINGEXPERIMENT I - NO MIXING PROVIDED

MODEL 1 - residence time in CSTR (τ_{CSTR}) = 36.5 seconds

- residence time in PFTR (τ_{PFTR}) = 22.8 seconds

<u>w</u> (rad/sec)	<u>wτ</u> <u>CSTR</u>	<u>CSTR</u> <u>angle</u>	<u>wτ</u> <u>PFTR</u>	<u>PFTR</u> <u>angle</u>	<u>TOTAL</u> <u>ANGLE</u>	<u>AMPLITUDE</u> <u>RATIO</u>
.01	.365	-20.1	.228	- 13	- 33.1	.94
.02	.730	-36.1	.456	- 26.1	- 62.2	.81
.03	1.095	-47.6	.684	- 39.1	- 86.7	.675
.04	1.460	-55.6	.912	- 52.2	-107.8	.565
.05	1.825	-61.3	1.140	- 65.2	-126.5	.48
.06	2.190	-65.5	1.368	- 78.3	-143.8	.415
.07	2.555	-68.6	1.596	- 91.3	-159.9	.364
.08	2.920	-71.1	1.824	-104.4	-175.5	.324
.09	3.285	-73.0	2.052	-117.4	-190.4	.291
.10	3.650	-74.7	2.280	-130.5	-205.2	.264



CSTR = 61.6% of total volume
 PFTR = 38.4% of total volume

TABLE V-2MODELINGEXPERIMENT I - NO MIXING PROVIDED

MODEL 2 - residence time in CSTR = 43 seconds
 - residence time in PFTR = 16.3 seconds

<u>w</u> <u>(rad/sec)</u>	<u>wτ</u> <u>CSTR</u>	<u>CSTR</u> <u>angle</u>	<u>wτ</u> <u>PFTR</u>	<u>PFTR</u> <u>angle</u>	<u>TOTAL</u> <u>ANGLE</u>	<u>AMPLITUDE</u> <u>RATIO</u>
.01	.43	-23.3	.163	- 9.3	- 32.6	.918
.02	.86	-40.7	.326	-18.6	-59.3	.758
.03	1.29	-52.2	.489	-28.0	-80.2	.614
.04	1.72	-59.8	.652	-37.3	-97.1	.502
.05	2.15	-65.0	.815	-46.6	-111.6	.422
.06	2.58	-68.8	.978	-56.0	-124.8	.362
.07	3.01	-71.6	1.141	-65.0	-136.6	.316
.08	3.44	-73.8	1.304	-74.2	-148.0	.28
.09	3.87	-75.5	1.467	-83.5	-159.0	.25
.10	4.30	-76.9	1.630	-93.0	-169.9	.227



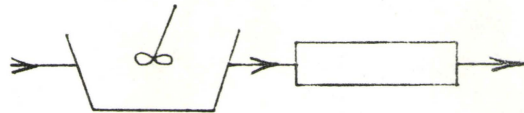
CSTR = 72.5% of total volume
 PFTR = 27.5% of total volume

TABLE V-3MODELINGEXPERIMENT II - NO MIXING PROVIDED

MODEL 3 - residence time in CSTR =57 seconds

- residence time in PFTR =56.5 seconds

<u>w</u> <u>(rad/sec)</u>	<u>wτ</u> <u>CSTR</u>	<u>CSTR</u> <u>angle</u>	<u>wτ</u> <u>PFTR</u>	<u>PFTR</u> <u>angle</u>	<u>TOTAL</u> <u>ANGLE</u>	<u>AMPLITUDE</u> <u>RATIO</u>
.01	.57	-29.7	.565	- 32.4	- 62.1	.87
.02	1.14	-48.8	1.130	- 64.8	-113.6	.66
.03	1.71	-59.7	1.695	- 97.0	-156.7	.506
.04	2.28	-66.3	2.260	-129.0	-195.3	.402
.05	2.85	-70.7	2.825	-162.0	-232.7	.331
.06	3.42	-73.7	3.390	-194.0	-267.7	.281
.07	3.99	-75.9	3.955	-226.0	-301.9	.244
.08	4.56	-77.6	4.520	-258.0	-335.6	.214
.09	5.13	-78.9	5.085	-290.0	-368.9	.191
.10	5.70	-80.1	5.650	-324.0	-404.1	.173



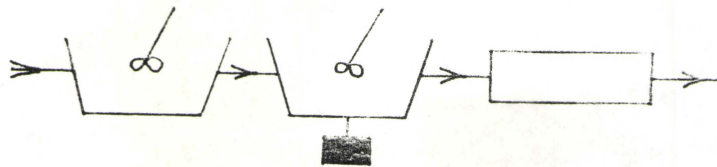
CSTR = 50.2% of total volume
 PFTR = 49.8% of total volume

TABLE V-4

MODELINGEXPERIMENT II - NO MIXING PROVIDED

- MODEL 4 - residence time in first CSTR = 37 seconds
 - residence time in second CSTR = 30 seconds
 - residence time in PFTR = 42 seconds
 - total residence time reduced by 4.5 seconds due to dead space

w (rad/sec)	FIRST CSTR		SECOND CSTR		w τ PFTR	PFTR angle	TOTAL ANGLE	AMPLITUDE RATIO	
	w τ	angle	w τ	angle				first	second
.01	.37	-20.3	.30	-16.7	.42	- 24	- 61.0	.935	.96
.02	.74	-36.5	.60	-31.0	.84	- 48	-115.5	.80	.86
.03	1.11	-48.0	.90	-42.0	1.26	- 72	-162.0	.68	.74
.04	1.48	-56.0	1.20	-50.2	1.68	- 96	-202.2	.56	.64
.05	1.85	-61.6	1.50	-56.3	2.10	-120	-237.9	.48	.56
.06	2.22	-65.8	1.80	-61.0	2.52	-144	-270.8	.41	.49
.07	2.59	-68.9	2.10	-64.5	2.94	-168	-301.4	.36	.43
.08	2.96	-71.3	2.40	-67.4	3.36	-192	-330.7	.32	.385
.09	3.33	-73.3	2.70	-69.7	3.78	-216	-359.0	.286	.347
.10	3.70	-74.8	3.00	-71.6	4.20	-241	-387.4	.261	.316



First CSTR = 32.6% of total volume
 Second CSTR = 26.5% of total volume
 PFTR = 37.0% of total volume
 Dead Space = 3.9% Of total volume

TABLE V-5MODELINGEXPERIMENT I - MIXING PROVIDEDMODEL 5 - residence time in CSTR = 45.5 seconds

- residence time in PFTR = 13.8 seconds

<u>w</u> (rad/sec)	<u>w T</u> CSTR	<u>CSTR</u> angle	<u>w T</u> PFTR	<u>PFTR</u> angle	<u>TOTAL</u> ANGLE	<u>AMPLITUDE</u> RATIO
.01	.455	-24.5	.138	- 7.9	- 32.4	.91
.02	.910	-42.3	.276	-15.8	- 58.1	.74
.03	1.365	-53.8	.414	-23.7	- 77.5	.59
.04	1.820	-61.2	.552	-31.6	- 92.8	.482
.05	2.275	-66.3	.690	-39.5	-105.8	.403
.06	2.730	-69.9	.828	-47.4	-117.3	.344
.07	3.185	-72.6	.966	-55.3	-127.9	.30
.08	3.640	-74.6	1.104	-63.2	-137.8	.265
.09	4.095	-76.3	1.242	-71.1	-147.4	.237
.10	4.550	-77.6	1.380	-79.0	-156.6	.215



CSTR = 76.7% of total volume
 PFTR = 23.3% of total volume

TABLE V-6MODELINGEXPERIMENT I - MIXING PROVIDEDMODEL 6 - residence time in CSTR = 41.7 seconds

- residence time in PFTR = 17.6 seconds

<u>w</u> (rad/sec)	<u>wτ</u> CSTR	<u>CSTR</u> angle	<u>wτ</u> PFTR	<u>PFTR</u> angle	<u>TOTAL</u> <u>ANGLE</u>	<u>AMPLITUDE</u> <u>RATIO</u>
.01	.417	-22.6	.176	- 10.1	- 32.7	.925
.02	.834	-39.8	.352	- 20.2	- 60.0	.768
.03	1.251	-51.4	.528	- 30.3	- 81.7	.625
.04	1.668	-59.0	.704	- 40.4	- 99.4	.515
.05	2.085	-64.4	.880	- 50.5	-114.9	.433
.06	2.502	-68.2	1.056	- 60.5	-128.7	.372
.07	2.919	-71.1	1.232	- 70.6	-141.7	.325
.08	3.336	-73.3	1.408	- 80.6	-153.9	.287
.09	3.753	-75.1	1.584	- 90.7	-165.8	.258
.10	4.170	-76.5	1.760	-101.0	-177.5	.233



CSTR = 70.3% of total volume
 PFTR = 29.7% of total volume

TABLE V-7MODELINGEXPERIMENT II - MIXING PROVIDEDMODEL 7 - residence time in CSTR = 87 seconds

- residence time in PFTR = 26.5 seconds

<u>w</u> (rad/sec)	<u>wτ</u> CSTR	<u>CSTR</u> angle	<u>wτ</u> PFTR	<u>PFTR</u> angle	<u>TOTAL</u> <u>ANGLE</u>	<u>AMPLITUDE</u> <u>RATIO</u>
.01	.87	-41.0	.265	- 15.2	- 56.2	.753
.02	1.74	-60.0	.530	- 30.4	- 90.4	.482
.03	2.61	-69.0	.795	- 45.5	-114.5	.35
.04	3.48	-74.0	1.060	- 60.7	-134.7	.276
.05	4.35	-77.0	1.325	- 76.0	-153.0	.225
.06	5.22	-79.2	1.590	- 91.1	-170.3	.189
.07	6.09	-80.7	1.855	-106.2	-186.9	.162
.08	6.96	-81.8	2.120	-121.4	-203.2	.142
.09	7.83	-82.7	2.385	-136.7	-219.4	.127
.10	8.70	-83.4	2.650	-152.0	-235.4	.114



CSTR = 76.6% of total volume
 PFTR = 23.3% of total volume

TABLE V-8MODELINGEXPERIMENT II - MIXING PROVIDED

- MODEL 8 - residence time in CSTR = 80 seconds
 - residence time in PFTR = 26.5 seconds
 - total residence time reduced by 7 seconds due to dead space

<u>w</u> (rad/sec)	<u>wτ</u> CSTR	<u>CSTR</u> angle	<u>wτ</u> PFTR	<u>PFTR</u> angle	<u>TOTAL</u> <u>ANGLE</u>	<u>AMPLITUDE</u> <u>RATIO</u>
.01	.80	-38.6	.265	- 15.2	- 53.8	.78
.02	1.60	-58.0	.530	- 30.4	- 88.4	.53
.03	2.40	-67.4	.795	- 45.5	-112.9	.385
.04	3.20	-72.6	1.060	- 60.7	-133.3	.298
.05	4.00	-76.0	1.325	- 76.0	-152.0	.242
.06	4.80	-78.2	1.590	- 91.1	-169.3	.204
.07	5.60	-79.8	1.855	-106.2	-186.0	.176
.08	6.40	-81.1	2.120	-121.4	-202.5	.154
.09	7.20	-82.1	2.385	-136.7	-218.8	.138
.10	8.00	-82.9	2.650	-152.0	-234.7	.124

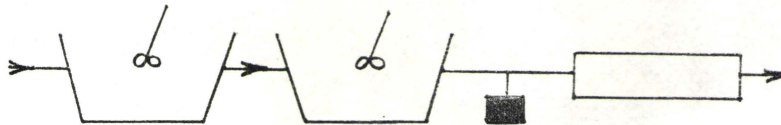


CSTR = 70.5% of total volume
 PFTR = 23.3% of total volume
 Dead Space = 6.2% of total volume

TABLE V-9MODELINGEXPERIMENT III - NO MIXING PROVIDED

- MODEL 9 - residence time in first CSTR = 22 seconds
 - residence time in second CSTR = 15 seconds
 - residence time in PFTR = 65 seconds
 - total residence time reduced by 7 seconds
 due to dead space

<u>w</u> (rad/sec)	<u>FIRST CSTR</u>		<u>SECOND CSTR</u>		<u>wτ</u> PFTR	<u>PFTR</u> angle	<u>TOTAL</u> <u>ANGLE</u>	<u>AMPLITUDE</u> <u>RATIO</u>	
	<u>wτ</u>	<u>angle</u>	<u>wτ</u>	<u>angle</u>				<u>first</u>	<u>second</u>
.01	.22	-12.4	.15	- 8.5	.65	- 37.2	- 58.1	.978	.99
.02	.44	-23.8	.30	-16.7	1.30	- 74.5	-115	.916	.96
.03	.66	-33.4	.45	-24.2	1.95	-112	-170	.835	.907
.04	.88	-41.4	.60	-31.0	2.60	-149	-221	.752	.858
.05	1.10	-47.7	.75	-36.8	3.25	-186	-271	.672	.80
.06	1.32	-52.8	.90	-42.0	3.90	-223	-318	.605	.744
.07	1.54	-57.0	1.05	-46.4	4.55	-260	-363	.545	.69
.08	1.76	-60.4	1.20	-50.2	5.20	-298	-409	.494	.642
.09	1.98	-63.2	1.35	-53.5	5.85	-335	-452	.451	.595
.10	2.20	-65.5	1.50	-56.3	6.50	-372	-494	.414	.55



First CSTR = 20.2% of total volume
 Second CSTR = 13.7% of total volume
 PFTR = 59.5% of total volume
 Dead Space = 6.6% of total volume